

Electromagnetic sum rules by spectral distribution methods

T. R. Halemane*

*Department of Physics and Astronomy, University of Rochester, Rochester, New York 14627
and Department of Physics and Astronomy, Rutgers University, Piscataway, New Jersey 08854*

J. B. French

Department of Physics and Astronomy, University of Rochester, Rochester, New York 14627

(Received 6 July 1981)

The spectral distribution methods are applied to calculate non-energy-weighted and linear-energy-weighted sum rules for electric and magnetic multipole excitations in the ds -shell nuclei ^{20}Ne , ^{24}Mg , ^{28}Si , ^{32}S , and ^{36}Ar . We see the inadequacy of ds -shell model space to explain the observed isoscalar quadrupole transition strengths. Isospin admixing of 1^+ levels in ^{24}Mg and ^{28}Si are also confirmed. For isovector $M1$, a detailed study of the Kurath sum rule is made. The strength sums for the higher order multipoles where experimental data are not accurate enough are also evaluated.

NUCLEAR STRUCTURE ^{20}Ne , ^{24}Mg , ^{28}Si , ^{32}S , ^{36}Ar ; sum rules for $E2$, $E4$, $M1$, $M3$, $M5$ transitions; Brown-Kuo Hamiltonian; spectral distribution methods used for calculation; Kurath sum rule extended.

I. INTRODUCTION

A statistical approach to nuclear structure calculations has been recently developed,¹⁻⁵ in part, to overcome a major practical limitation in the conventional shell-model approach. By dispensing with the need to know the nuclear wave functions, these statistical methods make it possible to handle calculations in large model spaces. The theory is based on the recognition of certain simplifying features arising out of the many-particle nature of the model spaces, by virtue of which, strengths and expectation values exhibit, in most cases, a smooth behavior (with small fluctuations) over the model space spectrum. Recently, the method was successfully applied to the study of beta-decay giant resonances⁶ and electromagnetic sum rules.⁷ We report here on the latter application.

A brief review of the spectral distribution method is given in Sec. II. In Sec. III we discuss the non-energy-weighted sum rules (NEWSR). The NEWSR is evaluated for electric and magnetic multipole excitations from the ground state in the ds -shell nuclei ^{20}Ne , ^{24}Mg , ^{28}Si , ^{32}S , and ^{36}Ar . A generally applicable procedure for evaluating the eigenvalue bound to the NEWSR is presented and numerical results obtained for the said excitations and nuclei. Comparisons are made with experimental data and shell-model results. By this sum-rule

analysis we are able to prove the known inadequacy of the ds -shell model space to explain the observed isoscalar quadrupole strengths in these nuclei. In addition, isospin admixing of 1^+ levels in ^{24}Mg and ^{28}Si are confirmed. The strength sums for the higher order multipoles, where experimental data is not accurate enough, are also predicted.

The linear-energy-weighted sum-rules (LEWSR) are discussed in Sec. IV. When the Hamiltonian is one body, this has a very simple form (expressible in terms of occupancies) and amounts to an extension of the Kurath sum rule to other types of excitations and to arbitrary one-body Hamiltonians. This is then extended to a unitary sum rule which takes account of a part of the two-body contribution to LEWSR, but can still be expressed in terms of occupancies. Further, the contribution to the LEWSR from the two-body interaction is fully evaluated. Comparisons are made with experimental data and with other theories. For isovector $M1$, a detailed study is made of the Kurath sum rule in the ds shell and the importance of the two-body contribution is established.

II. REVIEW OF SPECTRAL DISTRIBUTION METHODS

In a conventional nuclear shell-model⁸ calculation, one first generates the eigenvalues and eigen-

vectors of the Hamiltonian in a many-particle model space consisting of m particles distributed among N single-particle states with two-body interactions between the particles. Then the expectation values and strength functions of other operators of interest are calculated in the Hamiltonian eigenstates. All properties of the nuclear system in the chosen model space, and with the chosen interaction, are then defined, and one expects to get better and better results (as compared with experiment) by enlarging the model space and improving the model interaction. But, in practice, this soon becomes impossible since, even for relatively small values of m and N (and even if there are simplifying symmetries), the dimensionalities of the matrices to be constructed and diagonalized become too large to handle even for the most sophisticated computers.

The purpose of statistical nuclear spectroscopy¹⁻⁵ is to overcome this limitation by essentially starting at the other end of the problem. The idea is to look at the global properties of the Hamiltonian and other operators in the model space, and at the correlations between them. Some general properties of the system can be obtained most readily this way. Level densities and spectra can also be constructed from the moments. In fact, at least in finite-dimensional model spaces, one could in principle produce all the microscopic details by evaluating moments and covariances up to the order determined by the dimensionality of the model space. But this, by itself, would not be of much practical significance, if it were not for the existence of two helpful factors that contribute towards making this approach more successful than would be presumed otherwise.

The first simplifying factor derives from the recognition of the role played by a central limit theorem²⁻⁴ (CLT) in many-particle model spaces constructed by distributing nucleons over some finite set of single-particle states. Then, by virtue of this CLT, in the limit of large particle number, the smoothed eigenvalue distributions for most Hamiltonian operators in the model space become close to Gaussian. This, in turn, implies⁵ closely related characteristic asymptotic forms, for expectation values and strengths of other operators, defined by only a small number of traces over the model space of operators and their products. Such operator traces can be calculated^{3,9} by methods which do not involve construction of any Hamiltonian eigenfunctions. The fact that such traces can be obtained⁴ in a many-particle space by "propagation" from lower particle spaces is the second simplifying factor.

This requires one to evaluate those traces only in a minimum defining set of spaces of low particle or hole number. These two features make the statistical approach attractive, especially in model spaces of large dimensionality. Moreover, by its very nature, it gives results as more or less explicit functions of the Hamiltonian matrix elements so that one can easily connect the features of the Hamiltonian with the corresponding properties of the strengths and expectation values.

A. Polynomial expansions

Apart from the spectra and level densities, most calculations in statistical nuclear spectroscopy are based on two (usually rapidly convergent) polynomial expansions⁵; one for the expectation values and another for strengths.

Let H be the Hamiltonian for the nuclear system and O be an excitation operator which induces transitions $|W\rangle \xrightarrow{O} |W'\rangle$ between starting states $|W\rangle$ and final states $|W'\rangle$. Then the microscopic transition strength is defined as

$$R(W', W) = |\langle W' | O | W \rangle|^2. \quad (2.1)$$

The states $|W\rangle$ and $|W'\rangle$ may be in different eigensubspaces of H or the eigensubspaces may coincide. Let d and d' be their dimensionalities. It is also convenient to consider the eigenvalue densities $I(z)$ and $I'(z)$ in the initial and final subspaces. Also define

$$\rho(z) = d^{-1}I(z), \quad \rho'(z) = (d')^{-1}I'(z). \quad (2.2)$$

Associated with these densities are complete sets of orthonormal polynomials P_μ and P'_μ such that

$$\int P_\mu(x)P_\nu(x)\rho(x)dx = \delta_{\mu\nu}, \quad (2.3)$$

$$\delta(x-y) = \rho(x) \sum_\mu P_\mu(x)P_\mu(y), \quad (2.4)$$

with similar relations between ρ' and P'_μ . These polynomials¹⁰ can be constructed explicitly in terms of the density moments

$$\begin{aligned} M_p &= \int \rho(z)z^p dz = \langle H^p \rangle^m \\ &= \frac{1}{d} \langle\langle H^p \rangle\rangle^m, \end{aligned} \quad (2.5)$$

where we use the notation that, for any operator G , $\langle\langle G \rangle\rangle^m$ denotes the trace over the $|W\rangle$ model space and $\langle G \rangle^m$ denotes the average expectation value. The first two polynomials are

$$P_0(z)=1, P_1(z)=(z-\mathcal{E})/\sigma, \quad (2.6)$$

where $\mathcal{E}=M_1$ and $\sigma^2=M_2-M_1^2$ are the centroid and variance, respectively. The polynomial of order ν requires density moments of orders up to 2ν and is given by

$$[D_{\nu-1}D_\nu]^{1/2}P_\nu(z)=\begin{vmatrix} 1 & M_1 & M_2 & \cdots & M_\nu \\ M_1 & M_2 & & \cdots & M_{\nu+1} \\ \vdots & \vdots & & & \\ M_{\nu-1} & M_\nu & & \cdots & M_{2\nu-1} \\ 1 & z & z^2 & \cdots & z^\nu \end{vmatrix}, \quad (2.7)$$

where D_ν is the determinant in Eq. (2.7) with the last row replaced by $[M_\nu, M_{\nu+1}, \dots, M_{2\nu}]$.

When the density is Gaussian, i.e.,

$$\rho(W)=\frac{1}{\sqrt{2\pi\sigma^2}}\exp\left[-\frac{(W-\mathcal{E})^2}{2\sigma^2}\right], \quad (2.8)$$

the polynomials P_μ are related to the Hermite polynomials H_μ by

$$P_\mu(W)=(\mu!)^{-1/2}H_{e\mu}[(W-\mathcal{E})/\sigma], \quad (2.9)$$

where

$$H_{e\mu}(z)=2^{-\mu/2}H_\mu(z/\sqrt{2}).$$

When the density is of chi-squared type, the P_μ are related to the Laguerre polynomials.

In terms of the orthogonal polynomials $P_\mu(x)$, one derives

$$\begin{aligned} R(W',W) &= (I'(W)I(W))^{-1} \langle\langle O^\dagger \delta(H-W') O \delta(H-W) \rangle\rangle^m \\ &= (dd')^{-1} \sum_{\mu,\nu} \langle\langle O^\dagger P'_\mu(H) O P_\nu(H) \rangle\rangle^m P'_\mu(W') P_\nu(W) \end{aligned} \quad (2.10)$$

and similarly for the expectation value of an operator K ,

$$\begin{aligned} K(W) &= (I(W))^{-1} \langle\langle K \delta(H-W) \rangle\rangle^m \\ &= \sum_\nu \langle\langle K P_\nu(H) \rangle\rangle^m P_\nu(W). \end{aligned} \quad (2.11)$$

B. Central limit theorem

The above polynomial expansions would not be of much practical value if it were not for their rapid convergence. This results from the fact that, as we increase the number of particles, the model space eigenvalue density for "almost all" Hamiltonians goes² rapidly to Gaussian (by CLT). In the case of noninteracting particles this comes about because the density convolutes as we add particles. Thus, if we construct an m -particle system by adding one particle at a time and consider the energy of the state into which a particle is placed as a random variable, then the total energy is the sum of random variables and its density is given by the convolution of m single particle energy densities. The CLT then assures us that the convoluted density approaches Gaussian as the number of particles increases.

The convolution argument requires the variables to be additive and independent. These conditions are not met for a system of interacting nucleons.

The Pauli blocking effect (which can be ignored for dilute systems, i.e., $m \ll N$) violates statistical independence, and additivity is violated if interactions have to be considered. Despite all this, it is found that all nuclear Hamiltonians which give reasonable agreements with experimental data have model space spectra^{3,4} which are close to Gaussian. This is better understood by studying an ensemble of Hamiltonians of two-body interactions.^{11,12} It is found that the ensemble-averaged density is Gaussian and that for large systems ($1 \ll m \ll N$), only a negligible fraction of the members of the ensemble give deviant densities. However, in actual calculations, corrections to Gaussian are often necessary and will be incorporated.

In the CLT limit, Eqs. (2.10) and (2.11) can be approximated by⁵

$$K(W) = \langle K \rangle^m + \langle K(H-\mathcal{E}) \rangle^m \frac{(W-\mathcal{E})}{\sigma^2}, \quad (2.12)$$

$$R(W', W) = (d')^{-1} \left[\langle O^\dagger O \rangle^m + \langle O^\dagger (H - \mathcal{E}') O \rangle^m \frac{(W' - \mathcal{E}')}{(\sigma')^2} + \langle O^\dagger O (H - \mathcal{E}) \rangle^m \frac{(W - \mathcal{E})}{\sigma^2} \right. \\ \left. + \langle O^\dagger (H - \mathcal{E}') O (H - \mathcal{E}) \rangle^m \frac{(W' - \mathcal{E}') (W - \mathcal{E})}{\sigma'^2 \sigma^2} \right]. \quad (2.13)$$

Equation (2.12) and, in fact, (2.11) also can be derived by a linear-response theory.^{5,13} It can also be interpreted by a geometrical picture.⁵

Finally, it should be noted that there are operators, like J^2 , $Q \cdot Q$, and pairing, which do not have asymptotic Gaussian spectra.¹⁴ $Q \cdot Q$, in fact, has an asymptotic density which is chi-squared in five variables, and in general, the spectrum of an operator of the multipole form $T^\lambda \cdot T^\lambda$ is chi-squared in $(2\lambda + 1)$ variables, which becomes Gaussian when λ is large enough.

C. Configuration partitioning

Partitioning the model space into subspaces is often necessary to treat properly the exact symmetries conserved by a Hamiltonian. On the other hand, partitioning by other properly chosen nonexact symmetries can provide, as discussed below, a simple way to get better accuracy, especially when dealing with huge model spaces. For that purpose we could add high-order terms to the CLT results [Eqs. (2.12) and (2.13)] but these terms involve more complicated traces that rapidly become harder to evaluate. Configuration partitioning provides an easier solution.⁵ In this, the single-particle space is divided into orbits, say l in number. Then $\sum_{i=1}^l N_i = N$, where N_i is the number of states in

the i th orbit. Correspondingly, the m -particle space is divided into configurations defined, as usual, by assigning numbers of particles to the various orbits— m_i particles in the i th orbit—such that $\sum_{i=1}^l m_i = m$. Each configuration is then defined by a partition $\vec{m} \equiv [m_1, m_2, \dots, m_l]$ and additional attributes (like isospin T or angular momentum J) if any. For a properly-chosen partitioning, the configuration densities are to some extent localized in the spectrum and it is natural to introduce orthonormal polynomials for each configuration and produce the overall result by combining the contributions of all the configurations. Each configuration term looks after a part of the total spectrum and when many such configurations are present, one gets high accuracy even with low order polynomials. It is thus equivalent to going to considerably higher orders in the polynomial expansion over the entire model space. With configuration partitioning, Eqs. (2.10) and (2.11) can be replaced by⁵

$$K(W) = \sum_{\vec{m}} \frac{I_{\vec{m}}(W)}{I_m(W)} K(W; \vec{m}), \quad (2.14)$$

where

$$K(W; \vec{m}) = \sum_{\mu} \langle K P_{\mu}^{(\vec{m})}(H) \rangle_{\vec{m}} P_{\mu}^{(\vec{m})}(W) \quad (2.15)$$

and

$$R(W', m'; W, m) = \sum_{\vec{m}', \vec{m}} \frac{I_{\vec{m}'}(W') I_{\vec{m}}(W)}{I_{m'}(W') I_m(W)} R(W', \vec{m}'; W, \vec{m}), \quad (2.16)$$

where

$$R(W', \vec{m}'; W, \vec{m}) = (d_{\vec{m}})^{-1} \sum_{\mu, \nu} \langle O^\dagger(\vec{m}' - \vec{m}) P_{\mu}^{(\vec{m}')} (H) O P_{\nu}^{(\vec{m})} (H) \rangle_{\vec{m}} P_{\mu}^{(\vec{m}')} (W') P_{\nu}^{(\vec{m})} (W). \quad (2.17)$$

The superscripts and suffixes \vec{m} or \vec{m}' indicate that the corresponding quantities refer to or are evaluated in the configuration space \vec{m} or \vec{m}' , respectively. As the configuration traces are no harder to evaluate^{3,9} than the scalar ones, better accuracy is obtained in a simple way. It should also be remarked that in the configuration traces above, there is no restriction on the intermediate states. All the corre-

lations and interferences are thus properly included and the result is formally exact.

D. Unitary geometry and trace propagation

The $\binom{N}{m}$ states formed by distributing m fermions over N single-particle states form an irreducible rep-

resentation of the group $U(N)$ of unitary transformations in the single-particle space. This symmetry plays an important role in calculations because it provides simple methods for the evaluation of traces of operators.³ The trace operators in the m -particle space are scalars under this $U(N)$ group. Operators can be decomposed according to their unitary ranks $\nu=0,1,\dots,\frac{1}{2}N$ (where each ν corresponds, in the language of Young shapes, to a column structure $[N-\nu,\nu]$, or as is more commonly used, to a row structure $[2^\nu,1^{N-2\nu}]$). Then, a k -body operator $F(k)$ can be written as

$$F(k) = \sum_{\nu=0}^k F^\nu(k) = \sum_{\nu=0}^k \begin{bmatrix} n-\nu \\ k-\nu \end{bmatrix} F_k^\nu(\nu), \quad (2.18)$$

where $F^\nu(k)$ is the unitary¹⁵ rank- ν part of $F(k)$ and it has been further factored into its irreducible¹⁵ part $F_k^\nu(\nu)$ which is a ν -body operator derived from a k -body operator, as the subscript indicates. The binomial factor $\begin{bmatrix} n-\nu \\ k-\nu \end{bmatrix}$ converts $F_k^\nu(\nu)$ into a k -body operator. Then, for a $(0+1+\dots+u)$ -body operator, we have

$$\langle FG \rangle^m = \sum_{\nu=0}^{(u,v)_<} \sum_{k=\nu}^u \sum_{k'=\nu}^v \begin{bmatrix} m-\nu \\ k-\nu \end{bmatrix} \begin{bmatrix} m-\nu \\ k'-\nu \end{bmatrix} \begin{bmatrix} m \\ \nu \end{bmatrix} \begin{bmatrix} N-m \\ \nu \end{bmatrix} \begin{bmatrix} N-\nu \\ \nu \end{bmatrix}^{-1} \langle F_k^\nu G_{k'}^\nu \rangle^\nu, \quad (2.22)$$

where $(u,v)_<$ is the minimum of the pair. Without the $\nu=0$ term, Eq. (2.22) would give the covariance of F and G , viz., $\langle (F - \langle F \rangle)(G - \langle G \rangle) \rangle^m$.

These methods can be easily extended for configuration traces. Related methods for more complicated trace evaluation have been developed^{9,16,17} recently, and are expected to be important in the computation of higher-order traces.

E. Spectra and occupancies

From the smoothed eigenvalue density $\rho(W)$, it is not possible to extract the actual discrete spectra ex-

$$\rho(W) = \frac{\exp(-x^2/2)}{\sqrt{2\pi\sigma^2}} \left[1 + \frac{\gamma_3}{6}(x^3 - 3x) + \frac{\gamma_4}{24}(x^4 - 6x^2 + 3) \right], \quad (2.24)$$

where $x = (W - \mathcal{E})/\sigma$ and \mathcal{E} , σ , γ_3 , and γ_4 are the centroid, width, skewness, and excess, respectively, of the Hamiltonian H . When the model space is partitioned by configurations, $\rho(W)$ is taken to be a sum of configuration densities, each configuration density usually assumed to be a Gaussian.

The position of energy levels determined by these

$$F = \sum_{\nu=0}^u \sum_{k=\nu}^u \begin{bmatrix} n-\nu \\ k-\nu \end{bmatrix} F_k^\nu(\nu). \quad (2.19)$$

The $\nu=0$ part gives the centroid of F . The scalar product of two irreducible operators F^ν and G^ν is then

$$\langle F^\nu G^\nu \rangle^m = \begin{bmatrix} m \\ \nu \end{bmatrix} \begin{bmatrix} N-m \\ \nu \end{bmatrix} \begin{bmatrix} N-\nu \\ \nu \end{bmatrix}^{-1} \langle F^\nu G^\nu \rangle^\nu \delta_{\nu\nu'}, \quad (2.20)$$

where

$$\langle F^\nu G^\nu \rangle^\nu = \begin{bmatrix} N \\ \nu \end{bmatrix}^{-1} \sum_{\alpha,\beta} F_{\alpha\beta}^\nu G_{\alpha\beta}^\nu. \quad (2.21)$$

The defining ν -particle matrix elements $F_{\alpha\beta}^\nu$ and $G_{\alpha\beta}^\nu$ are related to those of F and G by contraction operators.³ (Here we have assumed F and G to have real matrix elements. Then the Hermitian property makes them symmetric too.) Then, we have for the scalar product of two operators F and G , of maximum particle ranks u and v , respectively,

actly, but the following prescription (Ratcliff¹⁸ procedure) gives the most probable positions of the energy levels. The energy E_i of the i th level is obtained by requiring that

$$d \int_{-\infty}^{E_i} \rho(W) dW = \sum_{j=1}^{i-1} d_j + \frac{d_i}{2}, \quad (2.23)$$

where d_j denotes the degeneracy of j th energy level and d is the total dimensionality. In view of the CLT, good results are obtainable, by assuming a four moment Gram-Charlier expansion for $\rho(W)$, viz.,

methods are found⁴ to deviate from their exact positions by within half a local level spacing.

The occupancy $n_r(W)$ of the r th orbit can be¹⁹ calculated by putting $K = n_r$ in Eq. (2.12). Better accuracy is obtained if the model space is partitioned into these orbits, because then in Eq. (2.15) only the $\mu=0$ term survives, and we get

$$n_r(W) = \frac{\sum_{\vec{m}} m_r I_{\vec{m}}(W)}{I_m(W)}, \quad (2.25)$$

where m_r denotes number of particles in the r th orbit corresponding to the configuration \vec{m} .

III. NON-ENERGY-WEIGHTED SUM RULES

The non-energy-weighted sum rule²⁰ (NEWSR) for the excitations generated by an excitation operator O acting on a state $|\alpha\rangle$ measures the expectation value $\langle \alpha | O^\dagger O | \alpha \rangle$. As pointed out by Hsu,²¹ it is bounded by the largest eigenvalue of the (positive definite) operator $O^\dagger O$ acting in the model space of the system. Such sum-rule results can be of use in assessing whether a given model space and a given interaction Hamiltonian would be adequate to explain experimentally measured transition strengths, the point being that the individual strength is dominated by the sum-rule quantity which in turn is dominated by the maximum $O^\dagger O$ eigenvalue. If the experimental measurement is larger than the maximum eigenvalue then one has to enlarge the model space.

In small model spaces the eigenvalues can be found by constructing and diagonalizing the $O^\dagger O$ matrices; in certain other cases (as with isoscalar $E2$ transitions within a single major shell) $O^\dagger O$ is equivalent to a Casimir operator whose eigenvalues may be taken to be known. However, we shall

present a generally applicable procedure for evaluating the maximum eigenvalue using spectral distribution methods.

These eigenvalue limits, being independent of the Hamiltonian, are useful only in cases where the individual strength, or at least the total strength originating in a given state, is large (as happens sometimes with $E2$ excitations). But in other cases this limit may not be very useful. In such situations we need to know the NEWSR (i.e., the $O^\dagger O$ expectation value) itself, which takes account of the fact that the strength distribution depends on the Hamiltonian. The spectral distribution method can be used to do this too.

We shall present below, in Secs. III B and III C, procedures for evaluating both the NEWSR and its eigenvalue bound. Then in Sec. III D we apply these methods to electromagnetic excitations in even-even self-conjugate ds -shell nuclei. Before we do all this, we give, in Sec. III A, a brief account of the NEWSR in the spherical tensor formalism. Finally, in Sec. III E, we discuss average strengths and units.

A. Sum rule analysis

Consider a nuclear transition from an initial state ($x\Gamma_i\mu_i$) to a final state ($y\Gamma_f\mu_f$). Let $\sum_{t=0}^1 O^\lambda$ be the excitation operator. We use a direct-product notation (of Ref. 20) here wherein $\Gamma \equiv (J, T)$, $\lambda \equiv (k, t)$, $\mu \equiv (M, \mathcal{S})$, $[\Gamma] \equiv (2J+1)(2T+1)$, and

$$U(\Gamma_1\Gamma_2\Gamma_3\Gamma_4;\Gamma_5\Gamma_6) \equiv U(J_1J_2J_3J_4;J_5J_6)U(T_1T_2T_3T_4;T_5T_6),$$

where x and y denote quantum numbers other than angular momentum and isospin. M and \mathcal{S} are the z -components of angular momentum J and isospin T , respectively. \mathcal{S}_i and \mathcal{S}_f would be the same for transitions in a given nucleus (as with examples in the next section) but we keep the generality for the present. We shall make use of the techniques of spherical tensors and Racah algebra.

Nuclear levels are degenerate with respect to the z -component M of angular momentum J and hence it is natural to define the transition strength (also called the reduced transition probability) $B(O^\lambda, x\Gamma_i \rightarrow y\Gamma_f)$ by averaging over the initial z components M_i and summing over the final ones. Thus,

$$\begin{aligned} B(O^\lambda, x\Gamma_i \rightarrow y\Gamma_f) &= [J_i]^{-1} \sum_{M_i M_f} |\langle \psi_{y\mu_f}^{\Gamma_f} | \sum_{t=0}^1 O^{k,t} | \psi_{x\mu_i}^{\Gamma_i} \rangle|^2 \\ &= [J_i]^{-1} [T_f]^{-1} \left[\sum_{t=0}^1 C_{\mathcal{S}_i \mathcal{S}_f}^{T_i t T_f} \langle y\Gamma_f | | O^{k,t} | | x\Gamma_i \rangle \right]^2, \end{aligned} \quad (3.1)$$

where the second equality obtained by using the Wigner-Eckart theorem involves double barred matrix elements (dbme) of O^λ . Here $t=0$ for isoscalar and $t=1$ for isovector excitations. Now let

$$B(O^\lambda, x\Gamma_i \rightarrow \Gamma_f) = \sum_y B(O^\lambda, x\Gamma_i \rightarrow y\Gamma_f). \quad (3.2)$$

This gives the total reduced transition probability from the level $x\Gamma_i$ in the initial nucleus to all the levels of

angular momentum Γ_f in the final nucleus. Further simplification can be obtained by using the spherical tensor formulas²⁰

$$\langle y\Gamma_f || O^\lambda || x\Gamma_i \rangle = (-1)^{\Gamma_f + \lambda - \Gamma_i} \langle x\Gamma_i || \bar{O}^\lambda || y\Gamma_f \rangle, \quad (3.3)$$

$$\begin{aligned} \sum_y \langle x\Gamma_i || \bar{O}^\lambda || y\Gamma_f \rangle \langle y\Gamma_f || O^{\lambda'} || x'\Gamma_i \rangle \\ = [\Gamma_f]^{1/2} \sum_{\Delta} (-1)^{\lambda + \lambda' - \Delta} U(\Gamma_i \lambda \Gamma_i \lambda' : \Gamma_f \Delta) \langle x\Gamma_i || (\bar{O}^\lambda \times O^{\lambda'})^\Delta || x'\Gamma_i \rangle. \end{aligned} \quad (3.4)$$

Then,

$$\begin{aligned} B(O^\lambda, x\Gamma_i \rightarrow \Gamma_f) = [J_i T_f]^{-1} \sum_{t=0}^1 \sum_{t'=0}^1 C_{\mathcal{F}_i \mathcal{F}_f}^{T_i t T_f} C_{\mathcal{F}_i \mathcal{F}_f}^{T_i t' T_f} \\ \times \sum_{\Delta} [\Gamma_f]^{1/2} (-1)^{\Gamma_f + \lambda' - \Gamma_i - \Delta} U(\Gamma_i \lambda \Gamma_i \lambda' : \Gamma_f \Delta) \langle x\Gamma_i || (\bar{O}^\lambda \times O^{\lambda'})^\Delta || x\Gamma_i \rangle, \end{aligned} \quad (3.5)$$

where $\lambda = (k, t)$ and $\lambda' = (k, t')$. For transitions from $\Gamma_i = (0, 0)$ this expression reduces to

$$B(O^\lambda, 0 \rightarrow \Gamma_f) = [t]^{-1} \langle x, 0 | O^\lambda \cdot O^\lambda | x, 0 \rangle \delta_{\lambda \Gamma_f}, \quad (3.6)$$

where we have used the Hermiticity property

$$\bar{O}^\lambda = (-1)^\lambda O^\lambda \quad (3.7)$$

and the relation

$$O^\lambda \cdot O^\lambda = (-1)^\lambda [\lambda]^{1/2} (O^\lambda \times O^\lambda)^0. \quad (3.8)$$

Then, Eq. (3.6) gives the NEWSR for transitions induced by the excitation operator O^λ from the initial state $x, \Gamma_i = (0, 0)$. We shall therefore be interested in the eigenvalues and expectation values of $O^\lambda \cdot O^\lambda$. The explicit construction of the excitation operators O^λ for electric and magnetic multipoles is given in Appendix A and the evaluation of $O^\lambda \cdot O^\lambda$ in the standard form,²⁰ from O^λ , is given in Appendix B.

B. Eigenvalue bounds

The eigenvalue densities of $O^\lambda \cdot O^\lambda$ are highly non-Gaussian.¹⁴ The skewness and excess of these operators are given in Table I. For example, $E2 (T=0) \cdot E2 (T=0)$ has a skewness of 0.96 and excess of 0.88 in the $(ds)^8$ space. By partitioning we approximate this density by a sum of configuration densities, each assumed to be a Gaussian. Thus, in the $(ds)^{m,T}$ model space, the eigenvalue density of $O^\lambda \cdot O^\lambda$ is assumed to be

$$I_{m,T}^{O^\lambda}(x) = \sum_{\bar{m}} I_{\bar{m},T}^{O^\lambda}(x), \quad (3.9)$$

$$\begin{aligned} I_{\bar{m},T}^{O^\lambda}(x) = \frac{d(\bar{m}, T)}{\sqrt{2\pi\sigma_{O^\lambda}^2(\bar{m}, T)}} \\ \times \exp \left\{ -\frac{[x - \mathcal{E}_{O^\lambda}(\bar{m}, T)]^2}{2\sigma_{O^\lambda}^2(\bar{m}, T)} \right\}, \end{aligned} \quad (3.10)$$

where $\mathcal{E}_{O^\lambda}(\bar{m}, T)$ and $\sigma_{O^\lambda}^2(\bar{m}, T)$ are the centroid

and variance of the eigenvalues of $O^\lambda \cdot O^\lambda$ in the configuration space (\bar{m}, T) , and $d(\bar{m}, T)$ is the dimensionality of this (\bar{m}, T) space. The highest eigenvalue χ_{O^λ} of $I_{m,T}^{O^\lambda}(x)$ is then evaluated by requiring that

$$\int_{\chi_{O^\lambda}}^{\infty} I_{m,T}^{O^\lambda}(x) dx = \frac{1}{2}. \quad (3.11)$$

The validity of a configuration-Gaussian approximation to a non-Gaussian density lies in the fact that each configuration density looks after a more or less localized region of the spectrum, and when the whole space is divided into many configurations, these many pieces of information combine rather well to reproduce the original density. Crudely speaking, one could compare this procedure to the process of approximating an irregular patch of area (in two dimensions) by a large number of tiny regular squares.

In Fig. 1, we plot the distribution function for $E2 (T=0) \cdot E2 (T=0)$ in the $(ds)^4, T=0$ space, along with the configuration-Gaussian approximation to it. The agreement is good except at the lower end

TABLE I. Skewness and excess parameters for $E\lambda \cdot E\lambda$ and $M\lambda \cdot M\lambda$ operators in $(ds)^m$ spaces [for isoscalar $M1$, the \vec{J} term has been left out—see Eq. (3.14)]. Owing to the hole \rightleftharpoons particle symmetry of these operators, the values for $(ds)^{16}$ and $(ds)^{20}$ are the same as those for $(ds)^8$ and $(ds)^4$, respectively, and hence are not tabulated.

m	Skewness					Excess				
	$E2$	$E4$	Isoscalar $M1$	$M3$	$M5$	$E2$	$E4$	Isovector $M1$	$M3$	$M5$
4	0.993	0.835	0.760	1.27	0.647	0.520	0.130	1.09	0.438	-0.137
8	0.957	0.846	1.37	1.31	0.568	0.664	0.241	0.908	0.386	-0.239
12	0.950	0.839	1.47	1.31	0.488	0.694	0.232	0.873	0.326	-0.277
m	$E2$	$E4$	Isoscalar $M1$	$M3$	$M5$	$E2$	$E4$	Isovector $M1$	$M3$	$M5$
4	1.18	0.864	-0.604	1.55	0.824	-0.118	0.231	1.85	0.071	-0.242
8	0.877	0.646	2.35	1.72	0.255	0.173	0.036	0.860	-0.125	-0.079
12	0.794	0.583	3.01	1.73	0.078	0.273	0.017	0.615	-0.215	-0.105

where the configuration-Gaussian approximation has a tail extending to the negative side. Our interest, however, is only at the upper end. In Table II we give the largest eigenvalues calculated by this method for $E\lambda \cdot E\lambda$ and $M\lambda \cdot M\lambda$ in the ds shell. In the $(ds)^{4,T=0}$ cases we also calculate exact values by shell model and, for isoscalar $E2$, by SU(3). Good agreement is found in all cases [except for isoscalar $M1$, for which the larger discrepancy is due to the fact that $M1(T=0) \cdot M1(T=0)$ being proportion-

al to S^2 (see ahead) has only three distinct eigenvalues in the $(ds)^{4,T=0}$ space].

C. Expectation values

The expectation value of $O^\lambda \cdot O^\lambda$ can be obtained by the polynomial expansion (2.11) or its CLT approximation (2.12) with $K = O^\lambda \cdot O^\lambda$. In a $(ds)^{m,T}$ model space, the first term of the expansion is $\langle O^\lambda \cdot O^\lambda \rangle^{m,T}$, which is the average total strength from a single state and gives the 0th approximation to the NEWSR. These values are tabulated in Table III, for electric and magnetic multipoles in the ds shell. The second term in the expectation value expansion,

$$\langle O^\lambda \cdot O^\lambda (H - \langle H \rangle^{m,T}) \rangle^{m,T} \frac{W - \langle H \rangle^{m,T}}{\sigma_H^2(m,T)},$$

takes account of the fact that the strength distribution depends on the Hamiltonian. It depends on the $O^\lambda \cdot O^\lambda$ component of H and gives a contribution which is proportional to the correlation coefficient between $O^\lambda \cdot O^\lambda$ and H . These correlation coefficients are given in Table IV. The ground state (see Table V) expectation values thus determined are given in Tables VI and VII.

We shall get even better accuracy for the expectation values by using the configuration partitioning technique described in Sec. II, with (\vec{m}, T) configurations and CLT approximation in each configuration. These are also given in Tables VI and VII.

D. Examples

We consider NEWSR for electric and magnetic multipole⁸ transitions from the ground state in

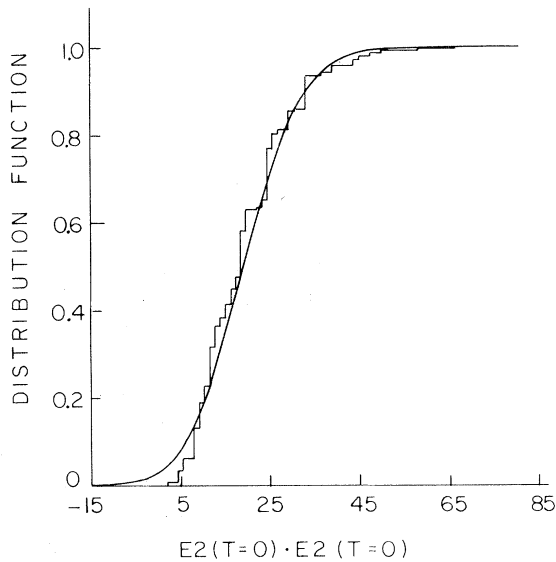


FIG. 1. The eigenvalue distribution function for $E2(T=0) \cdot E2(T=0)$ in the $(ds)^{4,T=0}$ space. The staircase curve is the exact distribution function obtained by a shell-model calculation and the other curve is the configuration-Gaussian approximation to it.

TABLE II. Upper bounds for the NEWSR of electric and magnetic transitions from the ground state in even-even self-conjugate nuclei. These are the largest eigenvalues of $O^\lambda \cdot O^\lambda$ when the excitation O^λ is isoscalar and of $\frac{1}{3}O^\lambda \cdot O^\lambda$ when the excitation is isovector [see Eq. (3.6)], and were obtained by the configuration-distribution method in $(ds)^{m,T=0}$ spaces. Also given (in parenthesis) are the bounds from the exact largest eigenvalues, calculated via SU(3) in the $E2$ case and via shell model in other cases. Units are $e^2 \text{fm}^{2L}$ for the electric (EL) cases and $\mu_N^2 \text{fm}^{2L-2}$ for the magnetic (ML) cases. All values should be multiplied by the corresponding scale factors given in the last row.

$m = A - 16$ $^A\text{Nucleus}$	Isoscalar					Isovector				
	$E2$	$E4$	$M1$	$M3$	$M5$	$E2$	$E4$	$M1$	$M3$	$M5$
^{20}Ne	62 (70)	73 (83)	35.6 (20.6)	20.3 (17.9)	4.9 (4.4)	50 (43)	54 (50)	46.5 (47.7)	29.0 (27.1)	9.5 (7.7)
^{24}Mg	125 (133)	174	76.1	38.0	8.3	95	121	80.8	52.8	16.1
^{28}Si	160 (179)	241	92.3	45.6	10.8	116	169	91.5	64.5	20.8
^{32}S	152 (161)	255	76.1	46.0	12.2	111	178	80.8	64.0	23.6
^{36}Ar	92 (103)	160	35.6	30.1	10.6	74	119	46.5	43.0	20.8
Scale factor	1	10^2	10^{-2}	10^2	10^5	1	10^2	1	10^3	10^6

even-even self-conjugate ds -shell nuclei. The Hamiltonian used is the Brown-Kuo (BK) interaction²² with experimental ^{17}O single-particle energies. The ground state energies are determined by the Ratcliff procedure¹⁸ and are given in Table V. The construction of the excitation operators O^λ and their scalar product $O^\lambda \cdot O^\lambda$ are discussed in an appendix. The upper bounds to NEWSR, obtained from the highest eigenvalues of $O^\lambda \cdot O^\lambda$ calculated in

$(ds)^{m,T=0}$ spaces using the statistical method of Sec. III B, are given in Table II. In some cases we also give, for comparison, the bounds obtained from the actual largest eigenvalues. The 0th approximation to the NEWSR are given in Table III. Given in Tables VI and VII are the NEWSR calculated using the CLT approximations in the scalar ($m, T=0$) and also the configuration ($\bar{m}, T=0$) spaces.

The experimental values of NEWSR, also given

TABLE III. Zeroth approximation to the NEWSR for electric and magnetic multipole excitations from the ground state in even-even self-conjugate ds -shell nuclei. These are the centroids of $[t]^{-1} O^\lambda \cdot O^\lambda$ in $(ds)^{m,T=0}$ spaces, where $t=0$ for isoscalar and $t=1$ for isovector excitations. The units are $e^2 \text{fm}^{2L}$ for the electric (EL) cases and $\mu_N^2 \text{fm}^{2L-2}$ for the magnetic (ML) cases. All values should be multiplied by the corresponding scale factors in the last row.

$m = A - 16$ $^A\text{Nucleus}$	Isoscalar					Isovector				
	$E2$	$E4$	$M1$	$M3$	$M5$	$E2$	$E4$	$M1$	$M3$	$M5$
^{20}Ne	19.5	26.5	10.1	5.57	1.38	16.7	22.7	14.3	11.0	3.37
^{24}Mg	35.2	54.0	16.2	10.1	2.81	30.1	46.3	22.9	19.8	6.90
^{28}Si	43.9	74.6	18.2	12.6	3.88	37.7	64.0	25.8	24.7	9.53
^{32}S	42.6	79.3	16.2	12.2	4.12	36.7	68.0	22.9	24.0	10.1
^{36}Ag	28.8	58.0	10.1	8.25	3.01	24.7	49.7	14.3	16.2	7.4
Scale factor	1	10^2	10^{-2}	10^2	10^5	1	10^2	1	10^3	10^6

TABLE IV. Correlation coefficients in the $(ds)^{m,T=0}$ spaces between the BK Hamiltonian and $O^\lambda \cdot O^\lambda$ for electric and magnetic excitation operators O^λ [for isoscalar $M1$, the \vec{J} term has been left out see Eq. (3.14)].

$m = A - 16$	Isoscalar					Isovector				
m	$E2$	$E4$	$M1$	$M3$	$M5$	$E2$	$E4$	$M1$	$M3$	$M5$
4	-0.523	-0.244	+0.012	-0.331	-0.378	+0.290	+0.208	+0.376	-0.273	-0.512
8	-0.557	-0.323	+0.172	-0.059	-0.112	+0.231	+0.137	+0.512	-0.015	-0.326
12	-0.552	-0.333	+0.195	+0.080	+0.134	+0.215	+0.116	+0.563	+0.145	-0.052
16	-0.519	-0.308	+0.161	+0.216	+0.382	+0.219	+0.121	+0.585	+0.289	+0.274
20	-0.431	-0.220	+0.010	+0.458	+0.644	+0.250	+0.159	+0.594	+0.471	+0.562

in Tables VI and VII, have been deduced from the data compiled in the literature. These data are from Refs. 23–27 for isovector $M1$ and from Ref. 28 for all others. We now turn to a more detailed discussion.

1. Electric quadrupole

In the isoscalar quadrupole case, along with the eigenvalue bound (to the NEWSR) calculated by the configuration-distribution method, we have also given (in Table II) the upper bounds from the exact largest eigenvalues calculated by the SU(3) model.²⁹ These are the values given in parenthesis under the isoscalar $E2$ column. They were obtained using the expression

$$e^2 b^4 \frac{5}{16\pi} [\lambda^2 + \mu^2 + \lambda\mu + 3\lambda + 3\mu - \frac{3}{4}L(L+1)]$$

for the eigenvalues of $E2(T=0) \cdot E2(T=0)$ when the model space is restricted to a single major shell. Here b is a scale parameter for the oscillator wave

TABLE V. Ground state parameters for even-even self-conjugate ds -shell nuclei. The ground state energy was determined by the configuration-distribution method (Ratcliff procedure) with $(\bar{m}, T=0)$ configurations. The Hamiltonian assumed is that of Brown-Kuo with ^{17}O single particle energies.

Nucleus	Active nucleons	Ground state		
	in ds shell	J	T	Energy
	m			
^{20}Ne	4	0	0	-40.1
^{24}Mg	8	0	0	-97.0
^{28}Si	12	0	0	-158.
^{32}S	16	0	0	-222.
^{36}Ar	20	0	0	-287.

functions; we have assumed the standard value $b^2 = 1.04 A^{1/3} \text{fm}^2$ in all of our calculations. For a given number of particles, the leading (λ, μ) representation defines the highest eigenvalue. For example, in $(ds)^{8,T=0}$ corresponding to ^{24}Mg , the exact largest eigenvalue of $E2(T=0) \cdot E2(T=0)$ from SU(3) is $133 e^2 \text{fm}^4$, whereas the spectral distribution method gives $125 e^2 \text{fm}^4$. In all cases, the latter method is seen to give values within 10% of the exact values. SU(3) and similar simple and exact methods are not usually available, in other kinds of model spaces and with other types of excitations, but the configuration-distribution method is no harder to apply to other cases.

We find that the ground state expectation values for $E2(T=0) \cdot E2(T=0)$ (see Table VI) are a large fraction of the largest eigenvalues (see Table II), a result of the high negative correlation (see Table IV) of this operator with the Hamiltonian. For example, the correlation coefficient in $(ds)^{12,T=0}$ is -0.56 and it takes the ground state expectation value to $102 e^2 \text{fm}^4$ from an average expectation value of $44 e^2 \text{fm}^4$. The corresponding maximum eigenvalue is $160 e^2 \text{fm}^4$ by spectral distribution method and $179 e^2 \text{fm}^4$ exact.

For purposes of comparison, we quote here the results of some exact shell-model calculations. In ^{20}Ne , Countee *et al.*,³⁰ get (with BK Hamiltonian) a value of $49 e^2 \text{fm}^4$ for the isoscalar quadrupole transition strength $B(E2, 0^+ \rightarrow 2_1^+)$ from the ground state to the first excited 2^+ state and very small (< 0.3) contributions to the higher lying 2^+ states. We get $43 e^2 \text{fm}^4$ for the NEWSR. The experimental value of $B(E2, 0^+ \rightarrow 2_1^+)$ is $292 e^2 \text{fm}^4$. McGroary and Wildenthal,³¹ using a suitably modified Kuo interaction and a truncated basis (with no more than four particles outside $d_{5/2}$ and no more than two in $d_{3/2}$) get a value of $79 e^2 \text{fm}^4$ for $B(E2, 0^+ \rightarrow 2_1^+)$ in ^{24}Mg and $74 e^2 \text{fm}^4$ in ^{28}Si . Our values for NEWSR using the BK Hamiltonian and

TABLE VI. NEWSR for isoscalar electric and magnetic multipole excitations from the ground state in even-even self-conjugate ds -shell nuclei. Values calculated by the scalar theory as well as by the more accurate configuration partitioning method [with $(\bar{m}, T=0)$ configurations] are given. The Hamiltonian assumed is that of Brown-Kuo with ^{17}O single-particle energies. Experimental values are also given where available, and include the strengths to levels below ~ 15 MeV excitation only. The units are $e^2\text{fm}^{2L}$ for the electric (EL) cases and $\mu_N^2\text{fm}^{2L-2}$ for the magnetic (ML) cases. All values should be multiplied by the corresponding scale factors given in the last column.

Nucleus \rightarrow		^{20}Ne	^{24}Mg	^{28}Si	^{32}S	^{36}Ar	Scale factor
$E2$	Scalar	36	79	102	92	50	1
	Config.	43	89	111	94	49	1
	Expt.	292 ± 36	518 ± 38	358 ± 22	387 ± 43	364 ± 42	1
$E4$	Scalar	35	85	122	123	76	10^2
	Config.	42	105	159	174	108	10^2
	Expt.						
$M1$	Scalar	9.8	7.3	5.8	7.8	9.9	10^{-2}
	Config.	9.3	4.1	1.3	3.8	8.7	10^{-2}
	Expt.		29.7 ± 11.5	2.41 ± 0.08	0.23 ± 0.07	1.73 ± 0.08	10^{-2}
$M3$	Scalar	8.7	11.4	10.2	6.3	1.6	10^2
	Config.	6.6	8.5	8.7	6.7	2.1	10^2
	Expt.						
$M5$	Scalar	2.3	3.3	3.1	1.6		10^5
	Config.	1.5	2.3	2.6	2.0	0.6	10^5
	Expt.						

TABLE VII. NEWSR for isovector electric and magnetic multipole excitations from the ground state in even-even self-conjugate ds -shell nuclei. Values calculated by the scalar theory as well as by the configuration partitioning method are given (except for isovector $M1$, where we give the 0th approximation to NEWSR—see text). The Hamiltonian assumed is that of Brown-Kuo with ^{17}O single-particle energies. Experimental values are also given where available, but include the strengths to levels below ~ 15 MeV excitation only. The units are $e^2\text{fm}^{2L}$ for the electric (EL) cases and $\mu_N^2\text{fm}^{2L-2}$ for the magnetic (ML) cases. All values should be multiplied by the corresponding scale factors given in the last column.

Nucleus		^{20}Ne	^{24}Mg	^{28}Si	^{32}S	^{36}Ar	Scale factor
$E2$	Scalar	9.6	18	22	22	15	1
	Config.	6.5	15	20	21	15	1
	Expt.			0.34	1.79	2.11	1
$E4$	Scalar	18	38	55	58	41	10^2
	Config.	19	43	65	75	57	10^2
	Expt.						
$M1$	0th approx.	14	23	26	23	14	1
	Expt.	2.04	5.81	6.68	6.50	3.11	1
$M3$	Scalar	15	20	20	15	6.7	10^3
	Config.	10	15	17	15	6.6	10^3
	Expt.						
$M5$	Scalar	5.9	9.5	10	6.8	1.2	10^6
	Config.	5.0	8.2	8.9	6.2	1.6	10^6
	Expt.						

the full ds -space are $89 e^2 \text{fm}^4$ for ^{24}Mg and $111 e^2 \text{fm}^4$ for ^{28}Si . The experimental values of $B(E2, 0^+ \rightarrow 2_1^+)$ are $486 e^2 \text{fm}^4$ in ^{24}Mg and $337 e^2 \text{fm}^4$ in ^{28}Si . And for ^{32}S , with an MSDI interaction and a truncated basis (not less than ten particles in $d_{5/2}$) Wildenthal *et al.*³² get a $B(E2, 0^+ \rightarrow 2_1^+)$ value of $54 e^2 \text{fm}^4$. We get $94 e^2 \text{fm}^4$ for the NEWSR and the experimental value is $387 e^2 \text{fm}^4$. In ^{36}Ar , Wildenthal *et al.*³³ get a $B(E2, 0^+ \rightarrow 2_1^+)$ value of $73 e^2 \text{fm}^4$ using a realistic interaction in the full ds -shell model space. Our value is $49 e^2 \text{fm}^4$ for the NEWSR and the experimental value is $364 e^2 \text{fm}^4$.

Experimental transition strengths for isoscalar quadrupole are seen to be much larger than the predicted NEWSR and their eigenvalue bounds. For example, the $0^+ \rightarrow 2^+$ transition connecting the two lowest states of ^{28}Si is experimentally determined to have a strength of $(337 \pm 15) e^2 \text{fm}^4$ while the upper bound for the NEWSR, calculated in $(ds)^{12, T=0}$, is $179 e^2 \text{fm}^4$. This proves that the ds -orbital space is inadequate. It has become customary to account for the large experimental $E2$ strength by the assumption of an effective charge, the justification being that the same effective charge works over a region of several nuclei. A proper treatment would, however, require enlarging the model space to include excitations across major shells. Such extended treatment would seem to be out of the question by any method except our own, and we propose to do such calculations in the future. We have not assumed here any effective charges in our calculations, and the values of other calculations quoted here have been corrected to discount any effective charges assumed by the original authors.

The isovector quadrupole strengths are known to be extremely fragmented and to lie at high excita-

tion energies. The experimental values of NEWSR quoted in Table VII include the contribution due to the lowest 2^+ , $T=1$ states only. Thus, in ^{28}Si the experimental value of transition strength from the ground state to the first 2^+ , $T=1$ level at 9.38 MeV is only $0.34 e^2 \text{fm}^4$, whereas the calculated value of the NEWSR is $20 e^2 \text{fm}^4$ and its eigenvalue bound is $116 e^2 \text{fm}^4$.

2. Magnetic dipole

The isoscalar magnetic dipole operator $M1$ ($T=0$) is $\sqrt{3/16\pi}[\vec{J} + (g_n + g_p - 1)\vec{S}]$, but the \vec{J} term does not contribute to the transitions that we consider. The \vec{J} term is much larger in magnitude than the \vec{S} term, and if it is not excluded, the fixed- T traces needed in the calculation are mostly determined by the diagonal contribution from the \vec{J} term. This amounts to adding nonexistent transition strength. This difficulty would not arise in fixed- JT model spaces (except for $\Delta J=0$, $J \neq 0$ transitions, in which case, the diagonal contribution can be eliminated by adding a term $\beta\vec{J}$ to the excitation operator so as to minimize the NEWSR quantity with respect to β). However, in the present case, dropping the \vec{J} term essentially removes the said difficulty, because, then the correlation coefficient between $M1(T=0) \cdot M1(T=0)$ and J^2 drops from very large to extremely small values. For example, in $(ds)^{12, T=0}$, this correlation coefficient is 0.94 when the \vec{J} term is included and 0.003 when it is left out.

Hence, we take

$$M1(T=0) \approx \sqrt{3/16\pi}(g_n + g_p - 1)\vec{S}. \quad (3.12)$$

The isovector $M1$ has the form

$$M1(T=1) = \sqrt{3/16\pi} \sum_i [-\vec{j}_i \vec{\tau}_i + (g_n - g_p + 1)\vec{s}_i \vec{\tau}_i]. \quad (3.13)$$

Since $(g_n + g_p - 1)^2 / (g_n - g_p + 1)^2 = 0.008$, the isovector $M1$ transitions are estimated to be about 100 times stronger than their isoscalar counterparts. We shall discuss more about this in Sec. III E.

For isoscalar $M1$, it is easy to calculate the eigenvalue bounds exactly. By Eq. (3.12)

$$M1(T=0) \cdot M1(T=0) = \frac{3}{16\pi} (g_n + g_p - 1)^2 S^2. \quad (3.14)$$

Then the maximum value of S in the model space

defines the upper bound for the NEWSR. In the examples, we consider S takes the maximum value of $w/2$, where w is the number of nucleons or holes (in the ds shell), whichever is smaller. This implies an upper bound of

$$\frac{3}{16\pi} (g_n + g_p - 1)^2 \frac{w(w+2)}{4}$$

for the NEWSR. These are tabulated below (in units of $10^{-2} \mu_N^2$, where μ_N is the nuclear magneton).

Nucleus	^{20}Ne	^{24}Mg	^{28}Si	^{32}S	^{36}Ar
upper bound (in $10^{-2}\mu_N^2$)	20.6	68.9	145	68.9	20.6

Thus, for ^{28}Si we get an upper bound of $1.45 \mu_N^2$ by this method and $0.92 \mu_N^2$ by the spectral distribution method (see Table II). The larger discrepancy seen here is, however, expected because S^2 has a spectrum that is highly degenerate (taking only three distinct eigenvalues in the ^{20}Ne and ^{36}Ar cases and going up to seven in the case of ^{28}Si), but the fact that even in this case the spectral distribution method gives bounds well within a factor of 2 compared to the exact ones is very encouraging (in many cases, a factor of 2 would be tolerable for such upper bounds).

These eigenvalue bounds are very large compared to the experimental values. For example, in ^{32}S the one observed $M1$ ($T=0$) transition to the ground state has a $B(M1, 0^+ \rightarrow 1^+)$ strength of $0.23 \times 10^{-2} \mu_N^2$ only. The eigenvalue bounds for the NEWSR in this case are $76 \times 10^{-2} \mu_N^2$ by the spectral distribution method and $69 \times 10^{-2} \mu_N^2$ exactly. It is then necessary to look at the NEWSR itself in order to get a better understanding. These are given in Table VI.

In ^{24}Mg , the $M1$ ($T=0$) \cdot $M1$ ($T=0$) centroid, i.e., the zeroth approximation to NEWSR, is $16 \times 10^{-2} \mu_N^2$. As the correlation coefficient with H is positive ($+0.17$), the value of NEWSR at the ground state is even lower and we obtain $7.3 \times 10^{-2} \mu_N^2$ by scalar and $4.1 \times 10^{-2} \mu_N^2$ by configuration calculations. The eigenvalue bound is $69 \times 10^{-2} \mu_N^2$. The experimental transition strengths are²⁸ $0.8 \times 10^{-2} \mu_N^2$ to the 7.75 MeV level and $29 \times 10^{-2} \mu_N^2$ to the 9.83 MeV level, thus exceeding the calculated NEWSR value, and also the larger zeroth approximation to it, but well within the eigenvalue bound. The large strength from the 9.83 MeV level suggests that³⁴ there is some isospin mixing due to the neighboring $J=1^+$, $T=1$ level at 9.97 MeV. (The 9.83 and 9.97 MeV levels in ^{24}Mg cannot both have $T=1$ because there is only one 1^+ analog state in the corresponding region of excitation energy in ^{24}Na .) Since the transition strength²⁴ to the 9.97 MeV level is $193 \times 10^{-2} \mu_N^2$, the mixing amounts to a Coulomb matrix element of 53 keV. If the experimental errors in the measurements corresponding to the 9.83 and 9.97 MeV levels are considered, this value could go down to 38 keV.

Isospin admixture has also been suspected²⁸ in ^{28}Si . The experimental values of $M1$ strengths are $0.12 \times 10^{-2} \mu_N^2$ and $2.3 \times 10^{-2} \mu_N^2$ to the $J=1^+$, $T=0$ levels at 8.33 and 10.73 MeV, respectively. The large $M1$ strength of the latter level suggests isospin admixing due to the neighboring $J=1^+$, $T=1$ level at 10.90 MeV which has an $M1$ strength of $113 \times 10^{-2} \mu_N^2$ from the ground state. This would amount to a Coulomb matrix element of 24 keV. The calculated values of NEWSR are $18 \times 10^{-2} \mu_N^2$ by zeroth approximation, $5.8 \times 10^{-2} \mu_N^2$ by scalar, and $1.3 \times 10^{-2} \mu_N^2$ by configuration calculations (the correlation coefficient with H is $+0.195$). This is quite compatible with isospin admixing—even if we allow for large inaccuracies that may arise in this case because the NEWSR value is small and far away (towards zero) from its value at the spectral centroid.

In ^{32}S the theoretical NEWSR is $3.8 \times 10^{-2} \mu_N^2$. Experimentally, for the one observed transition, $B(M1, 0^+ \rightarrow 1_1^+)$ is $0.23 \times 10^{-2} \mu_N^2$. Wildenthal *et al.*³² find, by a shell-model calculation, a $B(M1, 0^+ \rightarrow 1_1^+)$ strength of $0.27 \times 10^{-2} \mu_N^2$ in ^{32}S using an MSDI interaction. They did not calculate the NEWSR. The 1^+ levels at 7.00 MeV ($T=1$) and 7.19 MeV ($T=0$) are plausible candidates for isospin admixing, but there are no experimental measurements of transition rates corresponding to these.

In ^{36}Ar , the spin assignments are ambiguous. The 4.95 MeV level may be $J=1^+$ or $J=2^+$. Assuming $J=1^+$, the experimental $B(M1, 0^+ \rightarrow 1_1^+)$ strength is $1.73 \times 10^{-2} \mu_N^2$ compared to the calculated NEWSR value of $8.7 \times 10^{-2} \mu_N^2$. (The 2^+ assignment would mean a $E2$ strength of $16.8 e^2 \text{fm}^4$.)

For isovector magnetic dipole, the 0th approximation to the NEWSR are given in Table III. This value for ^{24}Mg is $23 \mu_N^2$, compared to the experimental NEWSR of $5.6 \mu_N^2$ (for two transitions). The $M1$ ($T=1$) \cdot $M1$ ($T=1$) operator is strongly and positively correlated with H with a correlation coefficient of $+0.51$ in $(ds)^{8, T=0}$. Because of this high positive correlation, the NEWSR at the ground state is expected to be considerably less than the 0th approximation and hence closer

to the experimental value. But the CLT approximations to the ground state NEWSR gives negative values ($-2.2 \mu_N^2$ in a scalar calculation and $-14.6 \mu_N^2$ in a configuration calculation), thus indicating that in this case it is necessary to consider the higher order terms of the polynomial expansions (2.11) and (2.15). This we shall investigate in the future.

3. Other multipoles

We also calculate the NEWSR and their eigenvalue bounds for $E4$, $M3$, and $M5$ transitions, both isoscalar and isovector. These are also given in Tables II, III, VI, and VII. The correlation coefficients with H are given in Table IV. $E4$ ($T=0$)- $E4$ ($T=0$) has a correlation coefficient of -0.33 with H in $(ds)^{12, T=0}$, and a largest eigenvalue of $2.4 \times 10^4 e^2 \text{fm}^8$. Its ground state expectation value is $1.6 \times 10^3 e^2 \text{fm}^8$. For isovector $E4$ the correlation coefficient is small and positive [0.12 in $(ds)^{12, T=0}$]. For $M3$ and $M5$, both isoscalar and isovector, the correlation coefficients with H are strongly dependent on the number of active nucleons, changing from negative values in the beginning of the shell to positive values at the upper end. For example, $M5$ ($T=0$)- $M5$ ($T=0$) has a correlation coefficient of -0.38 in $(ds)^{4, T=0}$ and $+0.64$ in $(ds)^{20, T=0}$.

The experimental strengths for $E4$, $M3$, and $M5$ are not known well enough for comparison with the calculated values. The branching ratios for them are indicated only by an upper limit, in the experimental literature; they cannot be measured accurately because of competing lower order electromagnetic transitions which are much stronger. Our calculations indicate that the actual branching ratios are expected to be several orders of magnitude smaller than the upper limits indicated in the experimental literature. For example, in ^{28}Si , the γ -ray branching ratio from the $4^+, T=0$ level at 4.62 MeV to the ground state is $^{28} < 0.5\%$ (and $\sim 100\%$ to the 2^+ state at 1.78 MeV) and since the mean lifetime $\tau_m = 59$ fs the transition strength $B(E4, 0^+ \rightarrow 4_1^+)$ is $< 47 \times 10^8 e^2 \text{fm}^8$. The theoretical value is only $1.6 \times 10^4 e^2 \text{fm}^8$ for the NEWSR and $2.4 \times 10^4 e^2 \text{fm}^8$ for its upper bound. The corresponding Weisskopf unit is $454 e^2 \text{fm}^8$. Similar situations are found in other nuclei and with $M3$ and $M5$ transitions.

E. Average strengths and units

The Weisskopf single particle unit³⁵ for the electric and magnetic multipole transitions is often

found to be too crude an estimate of the typical transition strengths in nuclei. For example, the Weisskopf unit for magnetic dipole transition has the value $1.79 \mu_N^2$, whereas the average experimental strengths are usually weaker by one or two orders of magnitude. A more realistic estimate of the typical magnitudes would be given by the average transition strength in the model space one is working in. This would also enable the shell effects to be taken into account in such a strength unit.

The average strength can be calculated by dividing the the NEWSR by the number of transitions. Using the NEWSR given in Tables VI and VII and taking the number of transitions to be the dimensionality³⁶ of the $\Gamma = \lambda$ subspace of $(ds)^m$, we tabulate, in Table VIII, the average strengths in the five ds -shell nuclei under consideration. For comparison purposes, the Weisskopf units are tabulated in Table IX. For example, in ^{24}Mg the average strength for isoscalar $E2$ is $0.74 e^2 \text{fm}^4$, whereas the Weisskopf unit is $4.11 e^2 \text{fm}^4$. For a given multipole the average strength is smaller in the middle of the shell than at either end.

The relative magnitudes of the different multipoles can also be inferred from the average strengths. Thus, the isovector $M1$ is seen to be stronger than isoscalar $M1$, by a factor of 100 in ^{20}Ne , 300 in ^{24}Mg , and 1000 in ^{28}Si . Isoscalar $E2$ is about ten times stronger than isovector $E2$ and isoscalar $E4$ is about five times stronger than isovector $E4$, in the midshell region. On the other hand, for $M3$ and $M5$, the isovector parts are stronger than the isoscalar ones, by a factor of 10 for $M3$ and 20 for $M5$.

The ratio of an individual transition strength to the average strength can be considered as a measure of collectivity for the transition. In Table X we give these values for the strongest of the observed transitions from the ground state for each multipole. Thus, the experimental $B(E2, 0^+ \rightarrow 2_1^+)$ of $486 e^2 \text{fm}^4$ in ^{24}Mg and $337 e^2 \text{fm}^4$ in ^{28}Si correspond to collectivities of about 6500 and 9900, respectively. Comparing different multipoles, isoscalar $E2$ is seen to be the most collective, isovector $M1$ coming next. The collectivities of the strongest nonadmixed isoscalar and isovector $M1$ transitions in ^{28}Si are 190 and 550, respectively.

IV. LINEAR-ENERGY-WEIGHTED SUM RULES

The linear-energy-weighted sum rules (LEWSR) are often used in the analysis of experimental data and theoretical models. But a generally applicable

TABLE VIII. Average strengths for electric and magnetic transitions in the ds shell. The units are $e^2 \text{fm}^{2L}$ for the electric (EL) and $\mu_N^2 \text{fm}^{2L-2}$ for the magnetic (ML) cases. All values should be multiplied by the corresponding scale factor in the last row.

$m = A - 16$	Isoscalar					Isovector				
${}^A\text{Nucleus}$	$E2$	$E4$	$M1$	$M3$	$M5$	$E2$	$E4$	$M1$	$M3$	$M5$
${}^{20}\text{Ne}$	77	96	30	15	6.3	9.9	38	26	14	15
${}^{24}\text{Mg}$	7.4	8.0	0.53	0.65	0.22	0.75	2.0	1.6	0.66	0.46
${}^{28}\text{Si}$	3.4	4.2	0.061	0.23	0.079	0.35	0.99	0.65	0.25	0.16
${}^{32}\text{S}$	7.8	13	0.49	0.51	0.19	1.1	3.5	1.6	0.66	0.35
${}^{36}\text{Ar}$	88	246	28	4.7	2.5	2.3	110	26	9.6	4.7
Scale factor	10^{-2}	1	10^{-4}	1	10^3	10^{-2}	1	10^{-2}	10	10^4

method to calculate the LEWSR has been lacking. The shell-model approach cannot be used (due to practical limitations) in large model spaces. Other approaches, like the classical sum rule³⁷ for electric multipoles and the Kurath³⁸ sum rule for isovector $M1$, have involved crude approximations.

We shall give here a quite general theory of LEWSR and then calculate it for electric and magnetic multipole transitions from the ground state in even-even self-conjugate ds -shell nuclei. When the Hamiltonian is one body, this has a very simple form, expressible in terms of ground-state occupancies, single-particle energies, and the double-barred matrix elements of the excitation operator. This amounts to an extension of the Kurath sum rule (which is for isovector $M1$ and for a one-body spin-orbit Hamiltonian) to other types of excitations and to arbitrary one-body Hamiltonians. We shall also discuss a unitary sum rule which takes account of a part of the two-body contribution, but

TABLE IX. Weisskopf units in $e^2 \text{fm}^{2L}$ for electric (EL) and $\mu_N^2 \text{fm}^{2L-2}$ for magnetic (ML) transitions. All values should be multiplied by the corresponding scale factors in the last row.

Nucleus	$E2$	$E4$	$M1$	$M3$	$M5$
${}^{20}\text{Ne}$	3.22	185	1.79	89.6	5.67
${}^{24}\text{Mg}$	4.11	301	1.79	114	9.22
${}^{28}\text{Si}$	5.05	454	1.79	140	13.9
${}^{32}\text{S}$	6.04	649	1.79	168	19.9
${}^{36}\text{Ar}$	7.06	888	1.79	196	27.2
Scale factor	1	1	1	1	10^3

can still be expressed in terms of occupancies. Further, we shall also evaluate the contributions to the LEWSR from the two-body interactions. Comparisons are also made with experimental data and with some shell-model results. For isovector $M1$, the relative importance of spin-flip and orbital contributions is examined explicitly.

The LEWSR operator is discussed in Sec. IV A and the applications to isovector magnetic dipole, isoscalar magnetic dipole, and electric quadrupole excitations are given in Secs. IV B, C, and D. Other multipoles are considered in Sec. IV E. In Sec. IV F, the strength centroids are evaluated using the NEWSR quantities calculated earlier in Sec. III.

A. The LEWSR operator

The linear-energy-weighted sum for the excitations $x\Gamma_i \xrightarrow{O^\lambda} \Gamma_f$ (using the notation of Sec. III and Ref. 20) generated by a one-body excitation operator O^λ is defined by [where $\lambda = (k, t)$, $\Gamma = (J, T)$]

TABLE X. Collectivities for the strongest observed transition from the ground state for each nucleus and multipole.

$m = A - 16$	Isoscalar		Isovector	
${}^A\text{Nucleus}$	$E2$	$M1$	$E2$	$M1$
${}^{20}\text{Ne}$	380			7.9
${}^{24}\text{Mg}$	6600	160		220
${}^{28}\text{Si}$	9900	190	98	550
${}^{32}\text{S}$	4200	46	170	220
${}^{36}\text{Ar}$	380	6.1	9.3	6.0

$$S_{EW} = [J_i]^{-1} \sum_y \sum_{M_i} \sum_{M_f} \left| \langle \psi_{y\mu_f}^{\Gamma_f} | \sum_{t=0}^1 O^{k,t} | \psi_{x\mu_i}^{\Gamma_i} \rangle \right|^2 (E_{y\Gamma_f} - E_{x\Gamma_i}). \quad (4.1)$$

Using the methods²⁰ of spherical tensors and Racah algebra, Eq. (4.1) can be rewritten as

$$S_{EW} = [J_i T_f]^{-1} \sum_{t=0}^1 \sum_{t'=0}^1 C_{\mathcal{F}_i \mathcal{F}_f}^{T_i t T_f} C_{\mathcal{F}_i \mathcal{F}_f}^{T_i t' T_f} (-1)^{\Gamma_f + \lambda - \Gamma_i} [\Gamma_f]^{1/2} \\ \times \sum_{\nu} (-1)^{\lambda + \lambda' - \nu} U(\Gamma_i \lambda \Gamma_i \lambda' : \Gamma_f \nu) \langle x \Gamma_i | | (\bar{O}^\lambda \times [H, O^{\lambda'}]_{-}^{\lambda'})^\nu | | x \Gamma_i \rangle, \quad (4.2)$$

where for any two spherical tensors T^λ and U^σ the commutator is defined by

$$[T^\lambda, U^\sigma]_{-}^\nu \equiv (T^\lambda \times U^\sigma)^\nu - (-1)^{\lambda + \sigma - \nu} (U^\sigma \times T^\lambda)^\nu. \quad (4.3)$$

The electric and magnetic multipole excitations are Hermitian [satisfying the condition $\bar{O}^\lambda = (-1)^\lambda O^\lambda$], and then the double barred expectation value in Eq. (4.2) can be replaced by

$$\frac{1}{2} \langle x \Gamma_i | | (\bar{O}^\lambda \times [H, O^{\lambda'}]_{-}^{\lambda'})^\nu - ([H, O^{\lambda'}]_{-}^{\lambda'} \times \bar{O}^\lambda)^\nu | | x \Gamma_i \rangle,$$

and if in addition $\Gamma_i = (0,0)$ we get

$$S_{EW} = \frac{1}{2} (-1)^\lambda [\lambda]^{1/2} [t]^{-1} \langle x, 0 | [O^\lambda, [H, O^\lambda]_{-}^\lambda]_0 | x, 0 \rangle. \quad (4.4)$$

Here $t=0$ for isoscalar and $t=1$ for isovector excitations. Since O^λ is one-body, the operator $[O^\lambda, [H, O^\lambda]_{-}^0]$ has the same particle rank as H itself. If H is of mixed particle rank, the p -body part of $[O^\lambda, [H, O^\lambda]_{-}^0]$ is determined by the p -body part of H only. Explicit construction of this double commutator operator when H is a $(1+2)$ -body operator is given in Appendix C. The contribution to S_{EW} in Eq. (4.4) from the one-body part of H has the simple form

$$S_{EW}^{(1)} = \sum_r e_r \langle x, 0 | n_r | x, 0 \rangle, \quad (4.5)$$

where $\langle x, 0 | n_r | x, 0 \rangle$ is the ground state occupancy of the r th orbit, and

$$e_r = [t]^{-1} \sum_b \alpha_{rb} \alpha_{br} (-1)^{r-b} [r]^{-1} (\epsilon_{bb} - \epsilon_{rr}). \quad (4.6)$$

Here for any r and b , ϵ_{bb} is the one-body energy in orbit b and α_{rb} is the double barred matrix element $\langle r || O^\lambda || b \rangle$. Moreover, $\sum_r [r] e_r = 0$.

A part of the two-body contribution to the expectation value in Eq. (4.4) can also be expressed in terms of occupancies by making a unitary decomposition of the operator $[O^\lambda, [H, O^\lambda]_{-}^\lambda]_0$. Noting that this operator is traceless in all m -particle spaces (and hence does not have a unitary rank zero part), we define the unitary sum by

$$S_{EW}^{v=1} = \sum_r \left[e_r + \frac{m-1}{N-2} \xi_r \right] \langle x, 0 | n_r | x, 0 \rangle. \quad (4.7)$$

When there is no radial degeneracy, this is all of the

unitary rank-one contribution. Here ξ_r is the traceless induced one-body matrix element of orbit r , defined (see Ref. 3) in terms of the standard two-body matrix elements V_{abcd}^Γ (see Appendix C) of $[O^\lambda, [H, O^\lambda]_{-}^\lambda]_0$ by (since the average induced one-body part vanishes)

$$\xi_r = \frac{1}{2} (-1)^\lambda [\lambda]^{1/2} [t]^{-1} \left[[r]^{-1} \sum_b [\Gamma] V_{rbrb}^\Gamma \right]. \quad (4.8)$$

We evaluate the ground state expectation value and occupancies appearing in Eqs. (4.4), (4.5), and (4.7) by the spectral distribution method using the configuration decomposition with fixed isospin ($T=0$). The Hamiltonian used is (BK) that of Brown-Kuo²² with ¹⁷O single-particle energies. For electric and magnetic multipole excitations in the ds shell, the parameters e_r and ξ_r are given in Table XI. The ground state occupancies are given in Table XII. We also tabulate the skewness, excess, and correlation coefficients with H of the LEWSR operator appearing in Eq. (4.4). These are given in Tables XIII and XIV.

B. Isovector magnetic dipole

The excitation operator is

$$M1(T=1) = \left[\frac{3}{16\pi} \right]^{1/2} \sum_i [-\vec{1}_i \vec{\tau}_i + (g_n - g_p) \vec{s}_i \vec{\tau}_i]. \quad (4.9)$$

TABLE XI. One-body and induced one-body parts of the LEWSR operator $\frac{1}{2}(-1)^\lambda[\lambda]^{1/2}[t]^{-1}[O^\lambda, [H, O^\lambda]_-]_0^0$ of Eq. (4.4) for isoscalar ($t=0$), isovector ($t=1$), and electric and magnetic multipole excitations (O^λ) in the ds shell. The values given are for ^{20}Ne and are to be multiplied by the corresponding scale factors in the last row. For the other even-even self-conjugate ds -shell nuclei of mass number A , multiply these ^{20}Ne values by $(A/20)^{L/3}$ for electric multipole (EL) and by $(A/20)^{(L-1)/3}$ for magnetic multipole (ML).

	<i>E2</i>	<i>E4</i>	<i>M1</i>	<i>M3</i>	<i>M5</i>	<i>E2</i>	<i>E4</i>	<i>M1</i>	<i>M3</i>	<i>M5</i>
$e_{5/2}$	4.21	27.5	6.99	0.546	0.0	4.21	27.5	8.58	3.48	0.0
$e_{3/2}$	-10.94	-41.2	-10.49	-0.032	0.0	-10.94	-41.2	-12.87	-2.97	0.0
$e_{1/2}$	9.24	0.0	0.0	-1.574	0.0	9.24	0.0	0.0	-4.50	0.0
$\xi_{5/2}$	6.26	14.3	3.62	1.828	0.0	6.26	14.3	4.46	6.23	0.0
$\xi_{3/2}$	-1.62	-21.4	-5.43	-0.016	0.0	-1.62	-21.4	-6.69	-1.55	0.0
$\xi_{1/2}$	-15.54	0.0	0.0	-5.446	0.0	-15.54	0.0	0.0	-15.59	0.0
Scale factor	1	10^2	10^{-2}	10^2	1	1	10^2	1	10^3	1

Excitations of nuclei using the 180° electron scattering technique³⁹ have been found to be very convenient for studying these transitions. The strengths of these transitions are usually discussed⁴⁰ in terms of the Kurath sum rule.

Kurath³⁸ made detailed studies of $1p$ -shell nuclei using the Hamiltonian

$$\mathcal{H} = \sum_i \mathcal{H}_0(i) + a \sum_i \vec{1}_i \cdot \vec{s}_i + \sum_{i>j} V(i,j), \quad (4.10)$$

which is a harmonic oscillator shell-model with spin-orbit coupling and two-body interactions of a central force nature. The relative strength a/K (where $K \sim 1$ MeV is a representative integral of the two-body interaction) of spin-orbit coupling was varied to study the effects and determine the best fits. A value of $a/K \approx 3$ in ^8Be and

$a/K \approx 4.5-6$ in ^{12}C were needed for the theoretical estimates to fit with experimental strengths.

The LEWSR for this model was then calculated by forming the double commutator [see Eq. (4.4)] between \mathcal{H} of Eq. (4.10) and $M1$ ($T=1$) of Eq. (4.9). The $\mathcal{H}_0(i)$ term commutes with the $M1$ ($T=1$) operator. The contribution from the spin-orbit term is

$$S_{\text{EW}}^{\text{Ku}} = \frac{3}{16\pi} a (g_p - g_n - 1)^2 \langle 0 | \sum_i \vec{1}_i \cdot \vec{s}_i | 0 \rangle. \quad (4.11)$$

Kurath found that for $4N$ nuclei the total calculated LEWSR was dominated by this spin-orbit contribution. Moreover, his calculations agreed well with the experimental data in p -shell nuclei. These conclusions were then extrapolated to ds -shell nuclei, although no corresponding shell-model studies

TABLE XII. The ground state occupancies of even-even self-conjugate ds -shell nuclei in the extreme single particle model and also those obtained by the configuration-distribution method [calculated in $(ds)^m, T=0$ model spaces] using the BK Hamiltonian.

$m = A - 16$	Extreme single particle model			Distribution method		
	$d_{5/2}$	$d_{3/2}$	$s_{1/2}$	$d_{5/2}$	$d_{3/2}$	$s_{1/2}$
$^4\text{Nucleus}$						
^{20}Ne	4	0	0	3.09	0.26	0.65
^{24}Mg	8	0	0	5.76	0.93	1.31
^{28}Si	12	0	0	8.14	1.77	2.09
^{32}S	12	0	4	10.21	2.84	2.95
^{36}Ar	12	4	4	11.63	4.65	3.73

TABLE XIII. Skewness and excess parameters in $(ds)^m$ spaces of the LEWSR operators [see Eq. (4.4)] for isoscalar and isovector, and electric and magnetic multipole from the ground states of even-even self-conjugate ds -shell nuclei.

$m = A - 16$ ${}^A\text{Nucleus}$	Skewness									
	Isoscalar		Skewness					Isovector		
	$E2$	$E4$	$M1$	$M3$	$M5$	$E2$	$E4$	$M1$	$M3$	$M5$
${}^{20}\text{Ne}$	0.380	-0.164	-1.06	-0.568	-0.763	-0.090	-0.221	-0.234	+0.031	+0.098
${}^{24}\text{Mg}$	0.223	-0.141	-0.819	-0.481	-0.667	-0.284	-0.255	-0.063	-0.207	-0.143
${}^{28}\text{Si}$	0.201	-0.127	-0.669	-0.428	-0.651	-0.314	-0.243	-0.027	-0.219	-0.184
${}^{32}\text{S}$	0.266	-0.094	-0.556	-0.350	-0.667	-0.266	-0.188	-0.051	-0.118	-0.143
${}^{36}\text{Ar}$	0.461	+0.014	-0.356	-0.132	-0.763	-0.044	-0.030	-0.081	+0.193	+0.098

$m = A - 16$ ${}^A\text{Nucleus}$	Excess									
	Isoscalar		Excess					Isovector		
	$E2$	$E4$	$M1$	$M3$	$M5$	$E2$	$E4$	$M1$	$M3$	$M5$
${}^{20}\text{Ne}$	+0.094	+0.232	+1.23	0.832	1.65	+0.055	-0.099	-0.430	-0.419	-0.043
${}^{24}\text{Mg}$	-0.200	+0.050	+1.05	0.208	0.462	-0.070	-0.196	-0.084	-0.106	-0.029
${}^{28}\text{Si}$	-0.192	-0.007	+0.755	0.112	0.248	-0.113	-0.249	-0.002	+0.013	-0.027
${}^{32}\text{S}$	-0.163	-0.068	+0.359	0.292	0.462	-0.107	-0.253	-0.112	0.079	-0.029
${}^{36}\text{Ar}$	+0.038	-0.250	-0.360	0.906	1.63	-0.060	-0.254	-0.428	+0.347	-0.043

were made.

In the ds shell, the Kurath sum S_{EW}^{Ku} of Eq. (4.11) can be written as

$$S_{EW}^{Ku} = \frac{3}{32\pi} a (g_p - g_n - 1)^2 (2n_{5/2} - 3n_{3/2})$$

$$= 4.286(2n_{5/2} - 3n_{3/2}) \mu_N^2 \text{ MeV} . \quad (4.12)$$

Here $n_{5/2}$ and $n_{3/2}$ are the ground state occupancies of the orbits $d_{5/2}$ and $d_{3/2}$, respectively, and we have used the commonly accepted value $a = 2.03$ MeV corresponding to the splitting of $d_{5/2}$ and $d_{3/2}$ levels as experimentally observed in ${}^{17}\text{O}$ spectra. This is then equivalent to the contribution $S_{EW}^{(1)}$ of Eq. (4.5) to the LEWSR from the one-body part of the BK Hamiltonian, because the $s_{1/2}$ orbit does not affect single-particle excitations of magnet-

ic dipole character (or, simply, $\langle f || M1 || s_{1/2} \rangle = 0$, unless $f = s_{1/2}$ and $\langle s_{1/2} || M1 || i \rangle = 0$, unless $i = s_{1/2}$).

Here we make a thorough study of the LEWSR for isovector magnetic dipole transitions from the ground state in even-even self-conjugate ds -shell nuclei. First, we calculate the Kurath sum rule using three sets of occupancies: (i) from the extreme single-particle model (j - j coupling), (ii) from the spectral distribution method using the BK Hamiltonian, and (iii) experimental occupancies^{41,42} (obtained from single-nucleon transfer reactions); the values are given in Table XV. S_{EW}^{Ku} is very sensitive to the occupancies. Thus, in ${}^{28}\text{Si}$, the Kurath sum rule is $103 \mu_N^2$ MeV in the extreme single particle limit, but goes down to $47 \mu_N^2$ MeV when the ground state occupancies obtained by the spectral distribution method are used. This compares favor-

TABLE XIV. Correlation coefficients in $(ds)^{m,T=0}$ spaces, between the BK Hamiltonian and the LEWSR operators [see Eq. (4.4)] for isoscalar and isovector, electric and magnetic multipole transitions from the ground states of even-even self-conjugate ds -shell nuclei.

$m = A - 16$ ${}^A\text{Nucleus}$	Isoscalar					Isovector				
	$E2$	$E4$	$M1$	$M3$	$M5$	$E2$	$E4$	$M1$	$M3$	$M5$
${}^{20}\text{Ne}$	-0.585	-0.745	-0.632	-0.622	-0.546	-0.680	-0.872	-0.754	-0.760	-0.762
${}^{24}\text{Mg}$	-0.552	-0.704	-0.578	-0.663	-0.584	-0.707	-0.881	-0.640	-0.729	-0.742
${}^{28}\text{Si}$	-0.556	-0.710	-0.587	-0.665	-0.579	-0.713	-0.887	-0.635	-0.708	-0.689
${}^{32}\text{S}$	-0.585	-0.745	-0.637	-0.643	-0.546	-0.711	-0.895	-0.691	-0.681	-0.586
${}^{36}\text{Ar}$	-0.663	-0.826	-0.749	-0.584	-0.459	-0.702	-0.909	-0.836	-0.631	-0.343

TABLE XV. Linear-energy-weighted sum rules for isovector magnetic dipole transitions from the ground state in some *ds*-shell nuclei. The values in parenthesis are from the (less accurate) scalar theory and are given for comparison purposes. The spin-flip contribution is the value of LEWSR obtained by excluding the $\vec{1}\vec{\tau}$ term in Eq. (4.9) for the isovector $M1$ operator. The units are μ_N^2 MeV.

Nucleus	Kurath sum rule			Unitary sum rule	Total LEWSR		
	Extreme single particle	Distribution method	Experimental occupancies		Distribution method	Experiment ^a	Spin-flip contribution
²⁰ Ne	34	23		25	67 (75)	23 ^d	38 (50)
²⁴ Mg	69	37	38 ^b	44	106 (126)	58 ^e	57 (80)
²⁸ Si	103	47	49 ^c	59	127 (152)	77 ^f	70 (96)
³² S	103	51		69	125 (148)	69 ^g	75 (96)
³⁶ Ar	51	40		58	91 (103)	33 ^h	61 (70)

^aSee Ref. 39.

^bSee Ref. 41.

^cSee Ref. 42.

^dSee Ref. 23.

^eSee Ref. 24.

^fSee Ref. 25.

^gSee Ref. 26.

^hSee Ref. 27.

ably with the value of $49 \mu_N^2$ MeV obtained by using the occupancies determined experimentally by Gove *et al.*⁴² from the ²⁸Si(*d*,³He)²⁷Al reaction. However, the total LEWSR is experimentally determined (by the known isovector $M1$ strengths) to be at least $77 \mu_N^2$ MeV, indicating substantial contributions from the two-body part of the Hamiltonian.

A part of the contribution from the two-body interaction to the LEWSR is included in the unitary sum rule $S_{EW}^{v=1}$ [see Eq. (4.7)] which have also been given in Table XV. The value is $59 \mu_N^2$ MeV for ²⁸Si and is also below the experimental value.

Thus, except in the extreme single-particle model (which is too crude, anyway), neither the Kurath sum rule nor its unitary extension is capable of explaining satisfactorily the experimental situation. We therefore calculate the total LEWSR, using the full (1 + 2)-body BK Hamiltonian. The calculations were made by configuration partitioning in fixed- $(m, T=0)$ spaces and the values are given in Table XV. Also given, for comparison purposes, are the values obtained by the less accurate scalar

theory. Thus, for ²⁸Si, the total calculated LEWSR is $127 \mu_N^2$ MeV (152 by scalar calculation) compared to the experimental value of at least $77 \mu_N^2$ MeV. The experimental measurements include transitions to a few low lying states only, and hence are expected to be somewhat lower than the theoretical result.

Finally, we estimate the relative importance of spin-flip and orbital contributions to the isovector $M1$ strengths. The spin-flip part is obtained by neglecting the $\vec{1}\vec{\tau}$ term in Eq. (4.9) for the $M1$ ($T=1$) operator. The values are tabulated in Table XV. Indeed, we find that the spin-flip contribution predominates. Thus, in ²⁸Si on neglecting the $\vec{1}\vec{\tau}$ term in Eq. (4.9) we get an LEWSR value of $70 \mu_N^2$ MeV compared to the value $127 \mu_N^2$ MeV obtained with the full operator. This means, assuming the spin-flip and orbital-flip contributions to be in phase (for otherwise, the orbital part would have to be unreasonably large; it could also be easily verified by a direct calculation), the spin-flip amplitude is about 0.74 of the total amplitude.

C. Isoscalar magnetic dipole

These transitions are generally weak because the neutron and proton spin contributions tend to cancel.³⁷ In this case also, the contribution $S_{EW}^{(1)}$ from the one-body part of H to the LEWSR can be expressed in a form similar to the Kurath sum rule. Since the \vec{J} term in the isoscalar $M1$ operator

$$\sqrt{3/16\pi}[\vec{J} + (g_n + g_p - 1)\vec{S}]$$

commutes with H , it is only the \vec{S} term that contributes, and with the parameter a chosen to represent the splitting of the single-particle levels $d_{5/2}$ and $d_{3/2}$, the one-body contribution can be written as

$$S_{EW}^{(1)} = \frac{3}{16\pi} a (g_n + g_p - 1)^2 \langle 0 | \sum_i \vec{I}_i \cdot \vec{s}_i | 0 \rangle$$

$$= 0.0350(2n_{5/2} - 3n_{3/2})\mu_N^2 \text{ MeV} . \quad (4.13)$$

We calculate $S_{EW}^{(1)}$ using the occupancies presented in Table XII and give the values in Table XVI. Also given there are the unitary sum $S_{EW}^{v=1}$ and the total LEWSR for isoscalar $M1$.

For example, in ²⁸Si, the one-body contribution to LEWSR is $0.33 \mu_N^2 \text{ MeV}$ ($0.84 \mu_N^2 \text{ MeV}$ in $j-j$

coupling) and the unitary rank-one part of the two-body contribution increases this to the unitary sum $S_{EW}^{v=1}$ value of $0.48 \mu_N^2 \text{ MeV}$. The total LEWSR is $0.50 \mu_N^2 \text{ MeV}$. The one-body contribution is seen to dominate the total LEWSR in all cases.

The experimental values given in Table XVI include the one or two observed transitions only and hence are not complete. However, the following conclusions can be made.

In ²⁴Mg, the total calculated value for the total LEWSR is $0.37 \mu_N^2 \text{ MeV}$ whereas the experimental value is $2.9 \mu_N^2 \text{ MeV}$, for which the 7.75 MeV level contributes $0.064 \mu_N^2 \text{ MeV}$ and the 9.83 MeV level contributes $2.83 \mu_N^2 \text{ MeV}$. As discussed in the NEWSR case (Sec. III), the 9.83 MeV level is suspected to have admixtures from the $T=1$ level at 9.97 MeV, thus accounting for its larger transition strength and hence larger energy-weighted strength.

In ²⁸Si, the 10.73 MeV level contributes²⁸ $0.247 \mu_N^2 \text{ MeV}$ and the 8.33 MeV level contributes $0.01 \mu_N^2 \text{ MeV}$ to LEWSR, the theoretical value of total LEWSR being $0.5 \mu_N^2 \text{ MeV}$. This is compatible with the isospin admixing of the 10.73 MeV ($T=0$) and 10.90 MeV ($T=1$) levels suggested by the NEWSR discussion.

TABLE XVI. Linear-energy-weighted sum rules for isoscalar magnetic dipole transitions from the ground state in some ds -shell nuclei. Values given in parenthesis are from a scalar calculation. The experimental values include the one or two observed transitions only and hence are not complete. The units are $\mu_N^2 \text{ MeV}$. The experimental data are from Ref. 28.

Nucleus	Extreme single particle	$S_{EW}^{(1)}$ Distribution method	$S_{EW}^{v=1}$	Total LEWSR	
				Distribution method	Expt.
²⁰ Ne	0.28	0.19	0.20	0.19 (0.42)	
²⁴ Mg	0.56	0.30	0.36	0.37 (0.76)	2.9 ± 1.1 ^b
²⁸ Si	0.84	0.38	0.48	0.50 (0.93)	0.26 ± 0.01 ^b
³² S	0.84	0.41	0.56	0.53 (0.91)	0.011 ± 0.003 ^a
³⁶ Ar	0.42	0.33	0.47	0.41 (0.63)	0.009 ± 0.004 ^a

^aFor one transition.

^bFor two transitions.

D. Electric quadrupole

The LEWSR for isoscalar and isovector electric quadrupole transitions are given in Table XVII. For the isoscalar quadrupole, the one-body contribution is a significant fraction of the total LEWSR. For example, in ^{28}Si , the one-body contribution $S_{\text{EW}}^{(1)}$ is $43 e^2 \text{fm}^4 \text{MeV}$ and the unitary rank-one part of the two-body contribution increases this to $S_{\text{EW}}^{v=1}$ value of $53 e^2 \text{fm}^4 \text{MeV}$. The total LEWSR is $164 e^2 \text{fm}^4 \text{MeV}$, calculated by the configuration partitioning method in $(ds)^{12, T=0}$. The scalar theory, which gives 165, is seen to be equally good. From the shell-model calculation of McGrory and Wildenthal³¹ (who used a suitably modified Kuo interaction and a truncated basis), the $0^+ \rightarrow 2_1^+$ isoscalar quadrupole transition contributes a value $131 e^2 \text{fm}^4 \text{MeV}$ to the LEWSR. As seen in Sec. III the experimental transition strengths are much larger than can be explained by any ds -shell calculation (thus proving the need to enlarge the model space), and hence give large values of LEWSR too.

For isovector quadrupole, the one-body and the unitary rank-one parts of the LEWSR are the same as for the isoscalar case. However, the total LEWSR is much larger. This is because $T=1$ lev-

els, in general, lie at higher excitation energies compared to $T=0$ levels. For ^{28}Si , the total LEWSR is $449 e^2 \text{fm}^4 \text{MeV}$, of which $43 e^2 \text{fm}^4 \text{MeV}$ is from the one-body part.

A commonly used linear-energy-weighted sum rule for electric multipole (EL) transitions is the classical quantity³⁷

$$S_{\text{EW}}^{\text{cl}}(\text{EL}, T) = \frac{A}{4} \frac{e^2 \hbar^2}{2m_p} \frac{L(2L+1)^2}{4\pi} \langle 0 | r^{2L-2} | 0 \rangle, \quad (4.14)$$

where $\langle 0 | r^{2L-2} | 0 \rangle$ is the ground state expectation value of r^{2L-2} . [The result is the same for both isoscalar and isovector electric multipole (EL) transitions from the ground state in even-even self-conjugate nuclei.] This result is obtained by assuming the two-body interaction $V(i, j)$ in the Hamiltonian

$$\sum_i \frac{-\hbar^2}{2m_p} \nabla_i^2 + \sum_{i < j} V(i, j)$$

to be local and neglecting velocity dependent and exchange forces. Then the only nonvanishing contribution to LEWSR is from the kinetic energy term

$$\frac{-\hbar^2}{2m_p} \sum_i \nabla_i^2$$

TABLE XVII. Linear-energy-weighted sum rules for isoscalar and isovector electric quadrupole transitions from the ground states of some ds -shell nuclei. The values in parenthesis are those obtained by a scalar calculation. $S_{\text{EW}}^{(1)}$, $S_{\text{EW}}^{v=1}$, and $S_{\text{EW}}^{\text{cl}}$ are common to both the isoscalar and isovector transitions. The experimental and shell-model values take into account transitions to the first few levels only. Except for ^{20}Ne , the Hamiltonians used in the shell-model calculations are different from the BK Hamiltonian we have used (see Sec. III for a brief account of the interactions and model spaces they used). No effective charges are assumed. The units are $e^2 \text{fm}^4 \text{MeV}$. The experimental data are from Ref. 28.

Nucleus	Extreme single particle	$S_{\text{EW}}^{(1)}$ Distribution method	$S_{\text{EW}}^{v=1}$	Isoscalar		Isovector	$S_{\text{EW}}^{\text{cl}}$	
				Total LEWSR	Shell model	Expt.		Total LEWSR
^{20}Ne	17	17	18	48 (57)	72 ^a	477 ± 60	152 (135)	2630
^{24}Mg	38	30	35	115 (123)	108 ^b	835 ± 63	337 (308)	3560
^{28}Si	63	43	53	164 (165)	131 ^b	756 ± 82	449 (408)	4600
^{32}S	120	54	66	174 (164)	106 ^c	987 ± 126	430 (382)	5750
^{36}Ar	65	48	58	101 (106)	136 ^d	724 ± 93	252 (217)	6990

^aSee Ref. 30.

^bSee Ref. 31.

^cSee Ref. 32.

^dSee Ref. 33.

TABLE XIX. Linear-energy-weighted sum rules for isoscalar and isovector $M3$ transitions from the ground state for some ds -shell nuclei. The values in parenthesis are those obtained by a scalar calculation. The units are $\mu_N^2 \text{fm}^4 \text{MeV}$. All values should be multiplied by the corresponding scale factors in the last row.

Nucleus	Extreme single particle	Isoscalar			Isovector			Total LEWSR
		$S_{EW}^{(1)}$	Distribution method	$S_{EW}^{\nu=1}$	$S_{EW}^{(1)}$	Distribution method	$S_{EW}^{\nu=1}$	
^{20}Ne	2.2	0.65	0.94	35.4 (22.9)	14	7	8	82 (75)
^{24}Mg	4.9	1.2	2.4	74.7 (57.9)	31	13	18	170 (164)
^{28}Si	8.2	1.4	3.5	89.2 (78.0)	52	17	27	216 (214)
^{32}S	0.35	1.1	3.5	68.7 (70.7)	33	19	31	191 (200)
^{36}Ar	0.19	0.49	1.6	26.9 (35.7)	18	15	24	94 (115)
Scale factor	10^2	10^2	10^2	10^2	10^3	10^3	10^3	10^3

TABLE XX. Linear-energy-weighted sum rules for isoscalar and isovector $M5$ transitions from the ground state for some ds -shell nuclei. The values in parenthesis are those obtained by a scalar calculation. The units are $\mu_N^2 \text{fm}^8 \text{MeV}$. All values should be multiplied by the corresponding scale factors in the last row. $S_{EW}^{(1)}$ and $S_{EW}^{\nu=1}$ are not given because they vanish.

Nucleus	Isoscalar total LEWSR	Isovector total LEWSR
^{20}Ne	16.5 (8.9)	36.8 (28.9)
^{24}Mg	36.7 (25.2)	87.5 (71.5)
^{28}Si	45.2 (36.9)	116 (98.3)
^{32}S	34.5 (35.0)	99.0 (88.4)
^{36}Ar	13.0 (16.8)	39.7 (38.3)
Scale factor	10^5	10^6

F. Strength centroids

The strength centroids are defined by the ratio LEWSR/NEWSR. In general, because of the nature of their use, larger inaccuracies are tolerable for sum rules than for strength centroids. Hence, although with the present accuracy of our calculations we have been able to do meaningful comparison with experiment as far as sum rules are concerned (some other existing sum rules are much more crude than ours), strength centroids are a different matter and require better accuracy. However, for completeness, we give a brief discussion of the strength centroids calculated with our sum rules, but exclude the magnetic dipole case where larger inaccuracies can be expected in the NEWSR.

When $O^\lambda \cdot O^\lambda$ is positively correlated with H , its ground state expectation value is below the $O^\lambda \cdot O^\lambda$ centroid (both the expectation value and the centroid are positive since $O^\lambda \cdot O^\lambda$ is a positive definite operator). The spectral distribution method actually estimates how many widths away from the centroid does this expectation value lie, and if it is far enough below the centroid to be a low value (as with isoscalar $M1$), even a small inaccuracy in the separation of the expectation value from the cen-

troid could lead to a large inaccuracy in the expectation value thus estimated. And in some extreme cases (like isovector $M1$) we may even get a negative value (in the CLT limit). It would then be necessary to include the higher order terms in the polynomial expansions. Detailed shell-model comparisons made by Draayer, French, and Wong⁵ indicate that terms up to fourth order would be sufficient to get good accuracy.

Another source of inaccuracy is that our calculations are with fixed (m, T) traces and not with fixed (m, J, T) ones. This amounts to an averaging over the various J values, and J being an exact symmetry, could sometimes lead to significant inaccuracies. But detailed studies made by Kar⁶ (for β decay) have shown that reasonably good results should be obtainable even without fixed J averaging. Although evaluation of fixed (m, J, T) traces are difficult at present, the theory has been worked out by French and Mugambi⁴³ and a computer code has been written by Loughheed and Wong.⁴⁴ We hope to be able to use it in the future. A related problem is that for isoscalar excitations, with fixed (m, T) spaces, the contributions

from the diagonal terms (which do not cause transitions) to the NEWSR cannot be properly eliminated (for isovector excitations they are automatically excluded because of fixed T).

The strength centroids we calculated are given in Table XXI. For isoscalar $E2$, if the assumption of effective charges is justified, one expects to get strength centroids in agreement with experiment even though the individual sums are not. We find a discrepancy of about 20% between theory and experiment [we expect even better accuracy when fixed (m, J, T) calculations are made]. The low values of strength centroids predict collectivity for these transitions and this, of course, is what is seen experimentally, with the lowest 2^+ , $T=0$ state carrying most of the transition strength.

V. CONCLUSION

The spectral distribution method is opposed in spirit to the conventional shell-model approach where the calculations are of a highly detailed nature, but strong approximations about the model

TABLE XXI. Strength centroids for the different multipoles. Given for each nucleus are (a) strength centroid by scalar theory, (b) strength centroid by configuration theory, (c) strength centroid by experiment, and (d) energy of the lowest experimentally seen level of the corresponding multipolarity. The units are MeV.

Nucleus		Isoscalar				Isovector			
		$E2$	$E4$	$M3$	$M5$	$E2$	$E4$	$M3$	$M5$
²⁰ Ne	a	1.58	5.63	2.62	3.9	14.1	19.1	5.16	4.9
	b	1.12	3.52	5.38	11.1	23.4	18.6	7.95	7.3
	c								
	d	1.63	4.25			10.27			
²⁴ Mg	a	1.56	5.49	5.08	7.61	17.4	21.9	8.12	7.5
	b	1.29	3.52	8.84	16.2	23.0	19.9	11.2	10.7
	c	1.61							
	d	1.37	4.12	5.24		10.06	9.52		
²⁸ Si	a	1.62	5.75	7.66	12.0	18.2	22.9	10.8	9.8
	b	1.48	3.60	10.2	17.5	22.8	19.6	12.6	13.1
	c	2.11							
	d	1.78	4.62	6.28		9.38		9.32	
³² S	a	1.77	6.45	11.2	22.3	17.3	22.9	13.7	13.0
	b	1.84	3.83	10.3	17.7	20.7	18.3	12.9	16.1
	c	2.55							
	d	2.23	4.46	5.41		7.12			
²⁶ Ar	a	2.14	7.99	22.3		14.0	21.6	17.2	
	b	2.05	4.55	13.0		16.8	17.3	14.2	
	c	1.99							
	d	1.97	4.41			6.61		7.34	

space and the model interaction are often made for practical reasons; instead, by disregarding some of the details, it seeks to extend the calculations to less restricted model spaces, at the same time keeping the essential physical content intact. This is achieved by making use of certain simplicities that exist in many-particle model spaces.

We have seen here some applications of this method to electromagnetic transition data in ^{20}Ne , ^{24}Mg , ^{28}Si , ^{32}S , and ^{36}Ar . The model space for these calculations was the full ds shell. So far there have not been any exact shell-model strength calculations in the full ds -shell model space for ^{24}Mg , ^{28}Si , and ^{32}S .

By calculations of the NEWSR and its upper bound, we were able to demonstrate the inadequacy of the ds -shell space to explain low-lying isoscalar $E2$ excitations in these nuclei. We could also predict isospin admixings of 1^+ levels in ^{24}Mg and in ^{28}Si . Moreover, we predicted the strength sums for the higher order multipoles where the experimental data are not yet accurate enough.

We made a detailed study of the Kurath sum rule in these ds -shell nuclei, and evaluated the corrections to it from the two-body interaction. This two-body contribution to LEWSR has not been evaluated before for ds -shell nuclei. We have also given "Kurath-type" sum rules for other multipoles. These were then extended to a unitary sum rule, which takes into account a part of the two-body interaction and then we evaluated the total LEWSR also.

Among the extensions and improvements of this work that we propose to do in the future are (1) extending the model space to allow for excitations across major shells—this cannot be done by the conventional approach—such extended calculations are necessary to treat properly the giant isoscalar quadrupole strengths; (2) including in the calculation, one or two higher order terms of the polynomial expansions—this would enable us to calculate the ground state expectation values with better accuracy, especially when $O^\lambda \cdot O^\lambda$ is positively correlated with H ; and (3) making the calculations with fixed (\bar{m}, J, T) traces—this would give better accuracy and also enable us to extend our calculations to initial

states with nonzero angular momentum.

This work was supported in part by grants from the Department of Energy and the National Science Foundation.

APPENDIX A: ELECTRIC AND MAGNETIC MULTIPOLE OPERATORS

For a nucleus consisting of A active nucleons, the electric multipole operator of order L is defined by³⁵

$$E^L = \sum_{i=1}^A e_i r_i^L Y^L(\Theta_i \phi_i),$$

where e_i is the charge on the i th nucleon (or its "effective charge"), (r_i, Θ_i, ϕ_i) are its spherical coordinates, and Y^L is the spherical harmonic of order L . In the isospin notation ($\tau_i = +1$ for neutron, -1 for proton), E^L can be broken up into isoscalar and isovector parts such that

$$E^L = E^{L,T=0} + E^{L,T=1},$$

where

$$E^{L,T=0} = \frac{e_p + e_n}{2} \sum_{i=1}^A r_i^L Y^L(\Theta_i \phi_i) 1_{\text{isospin}},$$

$$E^{L,T=1} = -\frac{e_p - e_n}{2} \sum_{i=1}^A r_i^L Y^L(\Theta_i \phi_i) \tau_i,$$

where e_p and e_n are the effective charges of proton and neutron, respectively.

The double barred matrix elements (dbme) of the one-body electric and magnetic multipole operators are obtained as follows. Each single particle state can be denoted by $|nlsjmtt_z\rangle$ (where $s = \frac{1}{2}$ and $t = \frac{1}{2}$ for all nucleons). It can be separated into radial, angular, and isospin parts,

$$|nlsjmtt_z\rangle = |nl\rangle |lsjm\rangle |tt_z\rangle.$$

[The notation used is the standard one with n, l, s, j, m, t , and t_z representing, respectively, the radial, orbital angular momentum, spin, total angular momentum ($j = l + s$), z component of total angular momentum, isospin, and z component of isospin quantum numbers.] Then, using properties of spherical tensors and Racah algebra one obtains³⁵

$$\langle n_f l_f s_f j_f t_f | | E^{L,T} | | n_i l_i s_i j_i t_i \rangle = \langle n_f l_f | r^L | n_i l_i \rangle (-1)^{j_f + l_i - 1/2} C_{000}^{l_f L l_i}$$

$$\times \left[\frac{(2L+1)(2l_f+1)(2j_f+1)(2j_i+1)}{16\pi} \right]^{1/2} W(l_f j_f l_i j_i; \frac{1}{2} L)$$

$$\times \begin{cases} (e_p + e_n)\sqrt{2}, & \text{for } T=0 \text{ (isoscalar)}, \\ -(e_p - e_n)\sqrt{6}, & \text{for } T=1 \text{ (isovector)}. \end{cases}$$

Similarly, the magnetic multipole operators are defined by

$$M^L = \mu_N \sum_i [\text{grad}_i r_i^L Y^L(\Theta_i \phi_i)] \cdot \left[e_i \frac{2l_i}{L+1} + g_i s_i \right],$$

which is then divided into isoscalar and isovector parts,

$$M^{L,T=0} = \mu_N \sum_{i=1}^A [\text{grad}_i r_i^L Y^L(\Theta_i \phi_i)] \cdot \left[(e_p + e_n) \frac{l_i}{L+1} + \frac{(g_p + g_n)}{2} s_i \right] 1_{\text{isospin}},$$

$$M^{L,T=1} = -\mu_N \sum_{i=1}^A [\text{grad}_i r_i Y^L(\Theta_i \phi_i)] \cdot \left[(e_p - e_n) \frac{l_i}{L+1} + \frac{(g_p - g_n)}{2} s_i \right] \tau_i,$$

so that

$$M^L = M^{L,T=0} + M^{L,T=1}.$$

Here $\mu_N = e\hbar/2m_p c$ is the nuclear magneton, l_i and s_i are the orbital and spin angular momenta of the i th particle, and g_p and g_n are the spin-gyromagnetic factors for proton and neutron, respectively (we assume the standard values $g_p = 5.5855$ and $g_n = -3.8256$). The dbme are then given by (see also Ref. 35),

$$\langle n_f l_f s_j f t | | M^{L,T} | | n_i l_i s_j i t \rangle = \langle n_f l_f | r^{L-1} | n_i l_i \rangle (-1)^{L-1} (2L+1) \left[\frac{(2j_f+1)(2j_i+1)(2l_f+1)(2L-1)}{L 16\pi} \right]^{1/2} F_T,$$

where

$$F_T = \left\{ \begin{aligned} & \frac{L}{L+1} \sqrt{j_i(j_i+1)(2j_i+1)} W(l_f \frac{1}{2} L - 1 j_i; j_f l_i) W(j_f j_i L - 1 1; L j_i) (e_p + e_n) \\ & + \sqrt{\frac{3}{2}} \left[L \frac{(g_p + g_n)}{2} - (e_p + e_n) \frac{L}{L+1} \right] \begin{bmatrix} l_f & \frac{1}{2} & j_f \\ l_i & \frac{1}{2} & j_i \\ L-1 & 1 & L \end{bmatrix} \sqrt{2}, \text{ for } T=0 \text{ (isoscalar)}, \end{aligned} \right.$$

and

$$F_T = \left\{ \begin{aligned} & -\frac{L}{L+1} \sqrt{j_i(j_i+1)(2j_i+1)} W(l_f \frac{1}{2} L - 1 j_i; j_f l_i) W(j_f j_i L - 1 1; L j_i) (e_p - e_n) \\ & - \sqrt{\frac{3}{2}} \left[L \frac{(g_p - g_n)}{2} - (e_p - e_n) \frac{L}{L+1} \right] \\ & \times \begin{bmatrix} l_f & \frac{1}{2} & j_f \\ l_i & \frac{1}{2} & j_i \\ L-1 & 1 & L \end{bmatrix} \sqrt{6}, \text{ for } T=1 \text{ (isovector)}. \end{aligned} \right.$$

The radial matrix elements $\langle n_f l_f | r^k | n_i l_i \rangle$ ($k=L$ for EL, $k=L-1$ for ML) are to be evaluated in the wave functions of a harmonic oscillator potential since they form the basis states in the shell model. The wave functions for a harmonic oscillator potential $U(r) = \frac{1}{2} M \omega^2 r^2$ are given by

$$| n l s j m t_z \rangle = R_{nl}(r) | l s j m \rangle | t_z \rangle,$$

where the radial part $R_{nl}(r)$ is

$$R_{nl}(r) = N_{nl} e^{-vr^2/2} r^l \mathcal{Y}_{nl}(vr^2),$$

with

$$\nu \equiv \frac{1}{b^2} \equiv \frac{M\omega}{\hbar}$$

(the standard value is $\nu=0.964^{-1/3} \text{ fm}^{-2}$). The eigenvalue corresponding to the above wave function is

$$E_{nl} = (2n + l + \frac{3}{2})\hbar\omega, \quad n = 0, 1, \dots$$

[for example, $n=0$ for $1d$, $n=1$ for $2s$ in the (ds) shell]. We also have

$$N_{nl}^2 = \frac{(2l + 2n + 1)!!(2\nu)^{l+3/2}}{2^n n! [(2l + 1)!!]^2} \sqrt{2/\pi}$$

and

$$\mathcal{Y}_{nl}(\rho) = \sum_{\mu} \begin{pmatrix} n \\ \mu \end{pmatrix} \frac{(2l + 1)!!}{(2l + 2 + 1)!!} (-2\rho)^{\mu}$$

Using the integrals

$$\int_0^{\infty} e^{-\nu r^2} r^{2l+2} dr = \begin{cases} \frac{(2l + 1)!!}{(2\nu)^{l+3/2}} \sqrt{\pi/2}, & \text{if } l \text{ is an integer,} \\ \frac{(2l + 1)!!}{(2\nu)^{l+3/2}}, & \text{if } l \text{ is half integer,} \end{cases}$$

we can readily obtain the following expression

$$\begin{aligned} \langle n_f l_f | r^k | n_i l_i \rangle &= \int R_{n_f l_f}(r) r^k R_{n_i l_i}(r) r^2 dr \\ &= \sum_{\mu_f=0}^{n_f} \sum_{\mu_i=0}^{n_i} (-1)^{\mu_f + \mu_i} \begin{pmatrix} 1 \\ 2\nu \end{pmatrix}^{k/2} \begin{pmatrix} n_f \\ \mu_f \end{pmatrix} \begin{pmatrix} n_i \\ \mu_i \end{pmatrix} \left[\frac{(2l_f + 2n_f + 1)!!(2l_i + 2n_i + 1)!!}{n_f! n_i! 2^{n_i + n_f}} \right]^{1/2} \\ &\quad \times \frac{(l_f + l_i + 2\mu_f + 2\mu_i + k + 1)!!}{(2l_f + 2\mu_f + 1)!!(2l_i + 2\mu_i + 1)!!} \begin{cases} 1, & \text{if } l_1 + l_2 + k \text{ is even,} \\ \sqrt{2/\pi}, & \text{if } l_1 + l_2 + k \text{ is odd.} \end{cases} \end{aligned}$$

APPENDIX B: SCALAR PRODUCT $O^\lambda \cdot O^\lambda$ OF TENSORIAL OPERATOR O^λ

We use the notation of Ref. 20. Let

$$O^\lambda = \sum_{r,s} \alpha_{rs} \mathcal{O}_{rs}^\lambda$$

be a one-body Hermitian [$\bar{O}^\lambda = (-1)^\lambda O^\lambda$, and hence $\alpha_{rs} = (-1)^{r-s} \alpha_{rs}$] operator of tensorial rank λ , where

$$\mathcal{O}_{rs}^\lambda = [\lambda]^{-1/2} (A^r \times B^s)^\lambda.$$

Here A^r and B^s are the creation and destruction ten-

sor operators for orbits r and s , respectively. We use a spin-isospin direct product notation²⁰ where $\Gamma \equiv (J, T)$, $(-1)^\Gamma = (-1)^{J+T}$, $[\Gamma] = (2J + 1) \times (2T + 1)$, and for the Racah W coefficients, $W(\Gamma_1 \Gamma_2 \Gamma_3 \Gamma_4; \Gamma_5 \Gamma_6) = W(J_1 J_2 J_3 J_4; J_5 J_6)$ $W(T_1 T_2 T_3 T_4; T_5 T_6)$, etc. Then, by the methods²⁰ of spherical tensors and Racah algebra, we can write $O^\lambda \cdot O^\lambda$ in the standard form

$$\begin{aligned} O^\lambda \cdot O^\lambda &= \sum_{r,s} \epsilon_{rs} [r]^{1/2} (A^r \times B^s)^0 \\ &\quad + \sum_{\substack{r \leq s \\ t \leq u \\ \Gamma}} [\Gamma]^{1/2} W_{rstu}^\Gamma (\Psi^\Gamma(r,s) \times \bar{\Psi}^\Gamma(t,u))^0. \end{aligned}$$

Here r, s, t , and u denote orbit labels and

$$\Psi^\Gamma(r, s) = -\zeta_{rs} (A^r \times A^s)^\Gamma,$$

$$\zeta_{rs} = \begin{cases} 1, & \text{if } r \neq s, \\ 1/\sqrt{2}, & \text{if } r = s. \end{cases}$$

We then get

$$\epsilon_{rs} = \frac{\sum \alpha_{pr}^2}{[r]} \delta_{rs},$$

$$W_{rstu}^\Gamma = \zeta_{rs} \zeta_{tu} [\beta_{rstu}^\Gamma - (-1)^{r+s-\Gamma} \beta_{srtu}^\Gamma - (-1)^{t+u-\Gamma} \beta_{rsut}^\Gamma + (-1)^{r+s-t-u} \beta_{srut}^\Gamma],$$

where $\beta_{rstu}^\Gamma = (-1)^{r+u-\Gamma} \alpha_{rt} \alpha_{su} W(rtsu : \lambda \Gamma)$. Because of symmetry relations among β_{rstu}^Γ , a further reduction is possible, giving finally

$$W_{rstu}^\Gamma = 2\zeta_{rs} \zeta_{tu} [\beta_{rstu}^\Gamma - (-1)^{r+s-\Gamma} \beta_{srtu}^\Gamma].$$

APPENDIX C: EVALUATION OF $[O^\lambda, [H, O^\lambda]_-]_-^0$

When O^λ is a one-body operator and H is a $(1+2)$ -body operator, $[O^\lambda, [H, O^\lambda]_-]_-^0$ is also a $(1+2)$ -body operator, with its one-body and two-body parts determined solely by the one-body and two-body parts, respectively, of H . We now express this double commutator operator in the standard form for $(1+2)$ -body operators. The notation used is that of Ref. 20. Let

$$O^\lambda = \sum_{a,b} \alpha_{ab} [\lambda]^{-1/2} (A^a \times B^b)^\lambda$$

and

$$\eta_{rs} = \delta_{rs} 2 \sum_b \alpha_{rb} \alpha_{br} (-1)^{r-b+\lambda} [\lambda]^{-1/2} [r]^{-1} (\epsilon_{bb} - \epsilon_{rr}),$$

$$V_{rstu}^\Gamma = \zeta_{rs}^2 \zeta_{tu}^2 [X_{rstu}^\Gamma - (-1)^{r+s-\Gamma} X_{srtu}^\Gamma - (-1)^{t+u-\Gamma} X_{rsut}^\Gamma + (-1)^{r+s-t-u} X_{srut}^\Gamma].$$

This step is for antisymmetrization, and the X_{rstu}^Γ appearing here are given by

$$X_{rstu}^\Gamma = [\lambda]^{-1/2} \{ T_1 + T_2 + T_3 + T_4 + T_5 + T_6 \},$$

where

$$T_1 = \sum_{i,j,\Omega} \alpha_{ri} \alpha_{ju} (-1)^{r+i+j+u+\Omega+\Gamma+\lambda} \zeta_{is}^{-1} \zeta_{tj}^{-1} W_{istj}^\Omega W(\lambda i \Gamma s : r \Omega) [\Omega] W(\Gamma t \lambda j : u \Omega) \zeta_{rs}^{-1} \zeta_{tu}^{-1},$$

$$T_2 = \sum_{i,j,\Omega} \alpha_{it} \alpha_{sj} (-1)^{\lambda+\Omega+\Gamma} [\Omega] \zeta_{iu}^{-1} \zeta_{rj}^{-1} W_{iurj}^\Omega W(\lambda i \Gamma u : t \Omega) W(\Gamma r \lambda j : s \Omega) \zeta_{rs}^{-1} \zeta_{tu}^{-1},$$

$$H = \sum_{r,s} \epsilon_{rs} [r]^{1/2} (A^r \times B^s)^0 + \sum_{\substack{rstu:\Gamma \\ r \leq s \\ t \leq u}} [\Gamma]^{1/2} W_{rstu}^\Gamma \times (\Psi^\Gamma(r, s) \times \bar{\Psi}^\Gamma(t, u))^0.$$

Here a, b, r, s, t , and u denote the orbit labels,

$$\Psi^\Gamma(r, s) = -\zeta_{rs} (A^r \times A^s)^\Gamma,$$

$$\zeta_{rs} = \begin{cases} 1, & \text{if } r \neq s, \\ 1/\sqrt{2}, & \text{if } r = s, \end{cases}$$

and a direct product spin-isospin notation is used, with

$$[r] \equiv 2(2j_r + 1),$$

$$(-1)^r \equiv (-1)^{j_r + 1/2},$$

etc., as in Appendix B. We also set

$$W_{rstu}^\Gamma = -(-1)^{r+s-\Gamma} W_{srtu}^\Gamma = -(-1)^{t+u-\Gamma} W_{rsut}^\Gamma = (-1)^{r+s-t-u} W_{srut}^\Gamma.$$

We then get, using the methods of spherical tensors and Racah algebra [see also Eqs. (3.10), (4.4), and (A5.16) in Ref. 20]:

$$[O^\lambda, [H, O^\lambda]_-]_-^0 = \sum_{r,s} \eta_{rs} [r]^{1/2} (A^r \times B^s)^0 + \sum_{\substack{rstu:\Gamma \\ r \leq s \\ t \leq u}} [\Gamma]^{1/2} V_{rstu}^\Gamma \times (\Psi^\Gamma(r, s) \times \bar{\Psi}^\Gamma(t, u))^0,$$

where (assuming no radial degeneracy),

$$T_3 = - \sum_{i,j} \alpha_{ri} \alpha_{sj} (-1)^{2r} \zeta_{rs}^{-1} \zeta_{ij}^{-1} W(\Gamma si \lambda : rj) W_{ijtu}^{\Gamma} f(t, u),$$

$$T_4 = - \sum_{i,j} \alpha_{it} \alpha_{ju} (-1)^{i+t+j-u} \zeta_{ij}^{-1} \zeta_{tu}^{-1} W_{ijrs}^{\Gamma} W(\Gamma ui \lambda : tj) f(r, s),$$

$$T_5 = - \sum_i \alpha_{ri} \alpha_{ir} (-1)^{r-i+\lambda} [r]^{-1} W_{rstu}^{\Gamma} \zeta_{rs}^{-2} f(t, u),$$

$$T_6 = - \sum_i \alpha_{it} \alpha_{ti} (-1)^{t-i+\lambda} [t]^{-1} W_{turs}^{\Gamma} \zeta_{tu}^{-2} f(r, s),$$

and

$$f(r, s) = \begin{cases} 1, & \text{if } r \leq s, \\ 0, & \text{otherwise.} \end{cases}$$

*Present address: Department of Physics, State University College, Fredonia, New York 14063.

- ¹J. B. French, in *Nuclear Structure*, edited by A. Hossain *et al.* (North-Holland, Amsterdam, 1967).
- ²J. B. French and K. F. Ratcliff, *Phys. Rev. C* **3**, 94 (1971); K. F. Ratcliff, *ibid.* **3**, 117 (1971); A. Gervois, *Nucl. Phys.* **A184**, 507 (1972).
- ³F. S. Chang, J. B. French, and T. H. Thio, *Ann. Phys. (N.Y.)* **66**, 137 (1971); F. S. Chang, University of Rochester Report UR-425, 1973 (unpublished).
- ⁴J. B. French, in *Dynamic Structure of Nuclear States*, edited by D. J. Rowe, L. E. H. Trainor, S. S. M. Wong, and T. W. Donnelly (University of Toronto, Ontario, Canada, 1972).
- ⁵J. P. Draayer, J. B. French, V. Potbhare, and S. S. M. Wong, *Phys. Lett.* **B55**, 263 (1975); **B55**, 349 (1975); J. P. Draayer, J. B. French, and S. S. M. Wong, *Ann. Phys. (N.Y.)* **106**, 472 (1977); **106**, 503 (1977).
- ⁶K. Kar, Ph.D. thesis, University of Rochester, 1979.
- ⁷T. R. Halemane, Ph.D. thesis, University of Rochester, 1979.
- ⁸A. de-Shalit and I. Talmi, *Nuclear Shell Theory* (Academic, New York, 1963); E. C. Halbert, J. B. McGrory, B. H. Wildenthal, and S. P. Pandya, in *Advances in Nuclear Physics*, edited by M. Baranger and E. Vogt (Plenum, New York, 1971), Vol. 4.
- ⁹S. Y. Li and D. S. Koltun (unpublished); V. Potbhare, Ph.D. thesis, University of Rochester, 1975; S. Ayik and J. N. Ginocchio, *Nucl. Phys.* **A221**, 285 (1974).
- ¹⁰H. Cramer, *Mathematical Methods of Statistics* (Princeton University, Princeton, New Jersey, 1946); G. Szego, *Orthogonal Polynomials* (American Mathematical Society Colloquium Publications, Providence, Rhode Island, 1939), Vol. XXIII.
- ¹¹J. B. French and S. S. M. Wong, *Phys. Lett.* **33B**, 449 (1970); **35B**, 5 (1971); O. Bohigas and J. Flores, *Phys. Lett.* **34B**, 261 (1971); **35**, 383 (1971); S. S. M. Wong and J. B. French, *Nucl. Phys.* **A198**, 188 (1972).
- ¹²K. K. Mon and J. B. French, *Ann. Phys. (N.Y.)* **95**, 90 (1975).
- ¹³F. S. Chang and J. B. French, *Phys. Lett.* **B44**, 131 (1973); **B44**, 135 (1973).
- ¹⁴M. Nomura, *Prog. Theor. Phys.* **48**, 442 (1972); J. B. French and J. P. Draayer, in *Group Theoretical Methods in Physics, Proceedings of the Seventh Internal Colloquium and Integrative Conference on Group Theory and Mathematical Physics*, edited by W. Beiglböck, A. Bohm, and E. Takasugi (Springer, Berlin, 1979); T. R. Halemane (unpublished).
- ¹⁵J. D. Louck, *Am. J. Phys.* **38**, 3 (1970).
- ¹⁶J. N. Ginocchio, *Phys. Rev. C* **8**, 135 (1973).
- ¹⁷B. D. Chang and S. S. M. Wong, *Nucl. Phys.* **A294**, 19 (1978).
- ¹⁸K. F. Ratcliff, *Phys. Rev. C* **3**, 117 (1971).
- ¹⁹V. Potbhare and S. P. Pandya, *Nucl. Phys.* **A256**, 253 (1976); J. P. Draayer, J. B. French, M. Prasad, V. Potbhare, and S. S. M. Wong, *Phys. Lett.* **57B**, 130 (1975).
- ²⁰J. B. French, in *Proceedings of the International School of Physics, Enrico Fermi, Course XXXVI*, edited by C. Bloch (Academic, New York, 1967).
- ²¹L. S. Hsu, *Phys. Lett.* **25B**, 588 (1967).
- ²²T. T. S. Kuo, *Nucl. Phys.* **A103**, 71 (1967).
- ²³W. L. Bendel, L. W. Fagg, S. K. Numrich, E. C. Jones, Jr., and H. F. Kaiser, *Phys. Rev. C* **3**, 1821 (1971).
- ²⁴L. W. Fagg, E. C. Jones, and W. L. Bendel, *Nucl. Instrum. Methods* **77**, 136 (1970).
- ²⁵L. W. Fagg, W. L. Bendel, E. C. Jones, Jr., and S. Numrich, *Phys. Rev.* **187**, 1378 (1969).
- ²⁶L. W. Fagg, W. L. Bendel, L. Cohen, E. C. Jones, Jr., H. F. Kaiser, and H. Uberall, *Phys. Rev. C* **4**, 2089 (1971).
- ²⁷L. W. Fagg, W. L. Bendel, E. C. Jones, Jr., L. Cohen, and H. F. Kaiser, *Phys. Rev. C* **5**, 120 (1972).
- ²⁸F. Ajzenberg-Selove, *Nucl. Phys.* **A190**, 1 (1972); P. M.

- Endt and C. Van der Leun, *ibid.* A214, 1 (1973).
- ²⁹J. P. Elliott, Proc. R. Soc. London A245, 128 (1958); A245, 562 (1958); M. Harvey, in *Advances in Nuclear Physics*, edited by M. Baranger and E. Vogt (Plenum, New York, 1968), Vol. I.
- ³⁰C. R. Countee, J. P. Draayer, T. R. Halemane, and K. Kar, Nucl. Phys. A356, 1 (1981).
- ³¹J. B. McGrory and B. H. Wildenthal, Phys. Lett. 34B, 373 (1971).
- ³²B. H. Wildenthal, E. C. Halbert, J. B. McGrory, and H. D. Graber, Phys. Rev. C 4, 1708 (1971).
- ³³B. H. Wildenthal, E. C. Halbert, J. B. McGrory, and T. T. S. Kuo, Phys. Rev. C 4, 1266 (1971).
- ³⁴O. Titze, Z. Phys. 220, 66 (1969).
- ³⁵P. J. Brussard and P. W. M. Glaudemans, *Shell-Model Applications in Nuclear Spectroscopy* (North-Holland, Amsterdam, 1977).
- ³⁶T. Sebe and M. Harvey, Atomic Energy of Canada Report AECL-3007, 1968.
- ³⁷E. K. Warburton and J. Wensler, in *Isospin in Nuclear Physics*, edited by D. H. Wilkinson (North-Holland, Amsterdam, 1969).
- ³⁸D. Kurath, Phys. Rev. 130, 1525 (1963).
- ³⁹L. W. Fagg, Rev. Mod. Phys. 47, 683 (1975).
- ⁴⁰S. S. Hanna, in *Isospin in Nuclear Physics*, edited by D. H. Wilkinson (North-Holland, Amsterdam, 1969); S. S. Hanna, in *Photonuclear Reactions*, edited by J. Ehlers *et al.* (Springer, Berlin, 1977); H. Uberall, R. A. Lindgren, and L. W. Fagg, Acta Phys. Austr. 41, 341 (1975).
- ⁴¹R. O. Nelson and N. R. Roberson, Phys. Rev. C 6, 2153 (1972).
- ⁴²H. E. Gove, K. H. Purser, J. J. Schwartz, W. P. Alford, and D. Cline, Nucl. Phys. A116, 369 (1968).
- ⁴³J. B. French and P. E. Mugambi (unpublished).
- ⁴⁴G. D. Lougheed and S. S. M. Wong, Nucl. Phys. A246, 29 (1975).